EFFECT OF DIFFERENTIAL ROUGHNESS ON FLOW CHARACTERISTICS IN A COMPOUND OPEN CHANNEL

by

NIRJHARINI SAHOO

A Thesis

submitted to

National Institute of Technology, Rourkela, India

in partial fulfilment of

the requirements for the degree of

MASTER OF TECHNOLOGY (RESEARCH)

In

CIVIL ENGINEERING

NATIONAL INSTITUTE OF TECHNOLOGY, ROURKELA

MAY, 2012

Certificate

This is to certify that the thesis entitled "**Effect of Differential Roughness on Flow Characteristics in a Compound Open Channel**" being submitted by Nirjharini Sahoo in partial fulfilment of the requirements for the award of **Master of Technology (Research)** in **Civil Engineering** to National Institute of Technology Rourkela, is a bona fide research carried out by her under our guidance and supervision.

The results embodied in this thesis have not been submitted, in part or full to any other University or Institute for the award of any degree or diploma.

Prof. K. K. Khatua   Prof. R. Jha

(Supervisor)   (Co-Supervisor)

Date: Date:

ACKNOWLEDGEMENTS

ABSTRACT

EFFECT OF DIFFERENTIAL ROUGHNESS ON FLOW CHARACTERISTICS IN A COMPOUND OPEN CHANNEL

Nirjharini Sahoo, M.Tech (R)

National Institute of Technology, Rourkela

Supervising Professors: Dr. K.K. Khatua and Dr. R. Jha

The present thesis is an outcome of a rigorous research effort undertaken by the author with a principal objective to observe the effect of differential roughness between the floodplains and the main channel on the flow characteristics of a compound channel having larger width ratio.

Generally the natural channels comprise a wider and rougher floodplain than the main channel (i.e. non-uniform boundary). In this case, much of the hydraulic resistance may be attributed to surface roughness and flow characteristics accounting for other forces. The resistance to flow along the channel boundary is manifested in the form of distribution of boundary shear along the periphery. From critical review of existing literature, it can be concluded that the boundary shear stress distribution is not uniform over the wetted perimeter of uniformly / non-uniformly roughened channel section. Still boundary shear distribution estimation in compound channel having width ratio greater than 10 along with roughness variation is rare to come across. Therefore, investigations which deals with the effect of wide floodplains and the differential roughness on evaluation of boundary shear distribution stress carried by the channel boundary is essential. In the present work, a series of experiments, for boundary shear stress on the wetted perimeter and stream-wise velocity at different points of the channel cross section grid, were carried out by using a pitot tube, for a compound channel having high width ratio of 15.75 with varying differential roughness (the ratio of base n value of floodplain surface roughness to that of main channel). The estimation of boundary shear stress was carried out by using well known Preston-tube technique preceding the estimation of boundary shear force distribution. Some commonly used equations of boundary shear distribution across the boundary of a compound channel were analyzed and tested with the experimental data. Then, a modified general expression to predict the boundary shear

distribution in compound channels having non-homogeneous roughness in the sub-sections was derived, which provided significant improvements in the results. The modified boundary shear distribution approach was tested for its validity using the fresh laboratory data collected for this purpose, as well as using the FCF data, Birmingham, UK, for a comparison. Analyses were also done to investigate the effect of differential roughness on depth-average velocity, flow distribution, and zonal and overall Manning's n variation to give substantial idea of a river system during overbank flow condition.

Key words: Boundary shear stress, Boundary shear distribution, Compound channel, Depth-average velocity, Manning's n, Preston-tube technique, Relative depth, Differential roughness, Width ratio.

TABLE OF CONTENTS

TABLE OF CONTENTS (Continued)

LIST OF FIGURES

LIST OF TABLES

NOTATIONS

α	Width ratio
β	Relative depth
γ	Differential roughness
δ	Aspect Ratio
ρ	Density of the flowing fluid
υ	Kinematic viscosity of fluid
τ	Mean boundary shear stress obtained by the energy gradient method
τ_0	Local shear stress
τ_e	Observed mean shear stress
τ_i	Shear stress on each point of the wetted perimeter of the channel boundary
Δp	Differential pressure
Δh	Difference in water elevation in the manometer,
θ	Angle of manometer with horizontal base
$\%SF_{fp}$	Percentage of shear force carried by floodplain
$\%Q_{mc}$	Percentage of flow in main channel
b	Width of main channel base
d	Diameter of priston tube
d'	Depth of flow
d_i	Particular size for which $i\%$ of the material by weight is finer than this size
d_{10}	Size for which 10% of the material by weight is finer than this size
d_{30}	Size for which 30% of the material by weight is finer than this size
d_{50}	Size for which 50% of the material by weight is finer than this size
d_{60}	Size for which 60% of the material by weight is finer than this size
d_{84}	Size for which 84% of the material by weight is finer than this size
f	Darcy–Weisbach's roughness coefficient

g	Gravitational acceleration
h	Depth of flow on the floodplain
h_1	Static pressure head in Manometer limb
h_2	Dynamic pressure head in Manometer limb
h_w	Height of water in the volumetric tank
k_s	Equivalent sand roughness
n	Overall Manning's roughness coefficient
n_{fp}	Manning's roughness coefficient of the floodplain boundary
n_{mc}	Manning's roughness coefficient of the main channel boundary
n_{zf}	Zonal roughness coefficient of floodplain
n_{zm}	Zonal roughness coefficient of main channel
p_i	Percentage of retained particles of d_i size
y	Lateral distance of the point (at which the U_d was measured) from the middle of the main channel towards floodplain wall
A	Aarea of channel cross section
A_{vt}	Aarea of the volumetric tank
B	Width of compound channel
C	Chezy's roughness coefficient
C_d	Coefficient of discharge of the notch
C_g	Coefficient of gradation
C_u	Coefficient of uniformity
D_g	Geometric mean diameter of the stone
F, F_1 and F_2	Functional relationships
G_s	Geometric standard deviation
H	Depth of flow on the main channel

H_n Height of water flow above the notch

L Length of the notch,

P Wetted perimeter of the channel section

Q_a Actual discharge

Q_e Experimental total discharge

Q_t Theoretical discharge

R Hydraulic radius of the channel cross section

S Bed Slope of the Channel / Energy gradient slope

S_g Specific gravity

SF Total shear force

SF_e Observed total shear force acted on the whole wetted perimeter

SF_{fp} Total shear force carried by the floodplains

SF_i Boundary shear force on each element of the wetted perimeter of the channel boundary

U Mean velocity

U_d Depth-averaged velocity

U_{mc} Zonal velocity of main channel

U_{fp} Zonal velocity of floodplain

U_p Velocity at a particular point

W_a Mean weight (in g) of the aggregate in the cylinder,

W_w Weight of water (in g) required to fill the cylinder

Y Half of the compound channel width

ABBREVIATIONS

FCF   Flood Channel Facility

AN   Angularity Number

SKM   Shiono & Knight Method

Chapter 1

INTRODUCTION

1 INTRODUCTION

A compound section of a natural channel generally comprises a wider and rougher floodplain than the main channel. The flow process in the open channel becomes more complicated at overbank stages due to the different hydraulic conditions prevailing in the main channel and the adjoining floodplains. For overbank stage, the resulting velocity distribution is generally not uniform across the cross-section; in particular the velocity tends to be higher in deeper main channel than the shallower floodplain, as in these compound channels the shallow floodplains offer more resistance to flow than the deep main channel. The velocity variation raise lateral momentum transfer between the deep main channel section and the adjoining shallow floodplains, which further complicates the flow process, leading to the uneven distribution of shear stress and flow in the main channel and floodplain regions (Sellin, 1964; Zheleznyakov, 1971; Myers and Elsawy, 1975; Rajaratnam and Ahmadi, 1979; Knight and Demetriou, 1983).

Because of the practical difficulty in obtaining sufficiently accurate and comprehensive field measurements of velocity and shear stress in compound channels under unsteady flood flow conditions (Bhowmik and Demissie, 1982), well designed laboratory investigations under steady flow conditions are still preferred as a trusted method to provide the information concerning the details of the flow structure. Such information is important in the application and development of numerical models aimed at solving certain practical hydraulic problems (i.e. to understand the mechanism of sediment transport, analysis of river migration, to prevent bank erosion in river channel, design stable channels, flood risk management, etc.).

Boundary shear, which has a vital role in estimating flow carrying capacity of a channel; sediment transportation; erosion of river, in compound channel have been studied by many previous investigators (Knight and Demetriou, 1983; Knight and Hamed, 1984; Wormleaton and Hadjipanos, 1985; Al-Khatib and Dmadi, 1999; Hin and Bessaih, 2004; Kean et al., 2009; Khatua et al., 2012). Still boundary shear distribution in compound channel having high width ratio along with roughness variation is rare to come across in literature.

The work presented in this dissertation is based upon a series of laboratory experiments in which a symmetrical compound channel having high width ratio was

roughened in such a way that its two floodplains had a greater roughness than that of the main channel. The differential roughness was changed in four different ways and the effect of differential roughness between the floodplain and the main channel on the flow characteristics in compound channel flow was studied.

1.1 Compound Channel with Non-Homogeneous Roughness

Rivers seldom bear a uniform roughness throughout its main channel and floodplain whether by nature or by manmade design. In a river, the floodplain may contain grass, trees, bushes, cultivated land, boulders etc. whereas main channel may contain gravel, sand which gives non-uniformity in surface roughness if we consider a compound section. Therefore, the effect of differential roughness on flow structure during overbank flow condition is retained here for environmental reasons. Some examples of compound rivers with different roughness are shown in (Fig. 1.1-1.2) and for better understanding a schematic diagram of inbank flow and overbank flow condition of a river section is shown in (Fig. 1.3 (a,b)).

Fig. 1.1 Godavari river, India [iii]   **Fig. 1.2 Indus river, Pakistan [iv]**

(a)

(b)
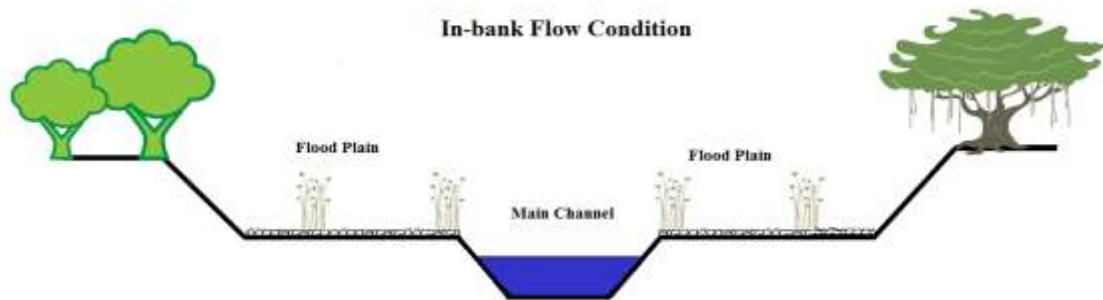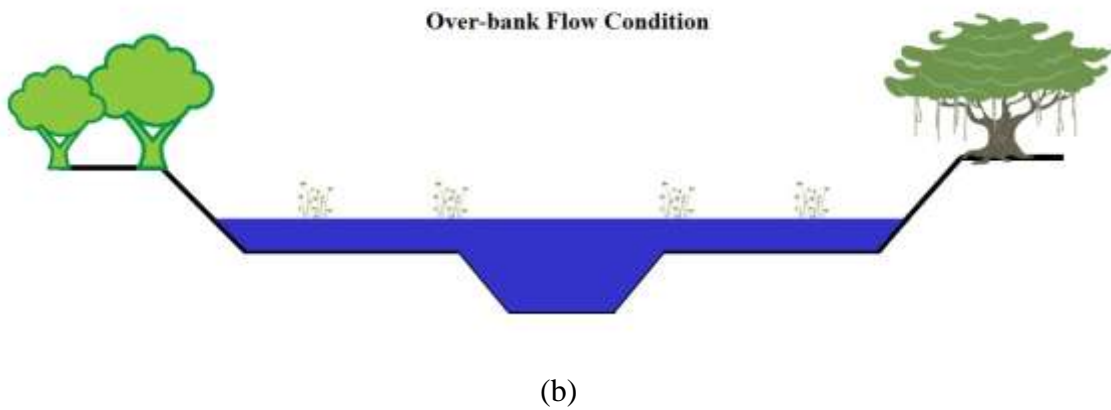
Fig. 1.3 Schematic daigram showing inbank and overbank flow condition in a river section

1.2 Differential Roughness

Since Manning's formula is simple in form and gives satisfactory result, it is the most convenient method of calculating resistance coefficient. It is mostly preferred for uniform flow in open channel. The base n value of bed material is generally used by river engineers for practical application in river engineering (Chow, 1959). In a river section, the roughness in main channel and floodplain is generally found to be dissimilar. The ratio of the base n value of main channel and that of floodplain is the differential roughness; whose influence on the flow characteristics during overbank flow has been studied in this research.

1.3 Scope and Approach of Present Study

Accurate predictions of boundary shear and discharge in compound channels has been the objective of many research efforts. Till date most experimental efforts have been concentrated on uniform roughness (smooth) compound channels constrained to low width ratio (width of compound channel / width of main channel base). Therefore, the present study intended to obtain information about the influencing capacity of differential roughness on flow structure (such as depth-averaged velocity, zonal and overall n, flow distribution, boundary shear distribution) in an idealised compound section having high width ratio. This research proposes a modified method for estimation of boundary shear distribution in a compound channel having high width ratio considering width ratio, relative depth and differential roughness as basic influencing parameter.

The present experimental study is pertains to natural channels having rougher floodplains than the main channel. For this study, data was obtained by conducting experiments at the Fluid Mechanics and Hydraulics Laboratory, N.I.T. Rourkela. The pre-existed straight compound channel made up of perspex sheet was roughened in three different ways so that we can get rougher floodplain than the main channel. The channel without any roughening work was considered as a channel of homogeneous roughness. The channel boundary was made rigid in all cases to make it appropriate for study of the influence of differential roughness on flow characteristics during overbank flow. In the first series experiment, the compound channel cross section was smooth (i.e. homogeneous surface). In the second series, the floodplain was roughened by putting woven wire mesh (from local market) and the main channel kept smooth. In the third series, the floodplain was roughened by crushed stone (from local market) and the main channel was roughened by the wire mesh. In fourth series, the floodplain was kept stone roughened and the main channel made smooth. These were considered as some representative of natural channel having rougher wider floodplain than its main channel.

1.4   Objectives of the Research Work

➤ To carry out laboratory experiments to investigate the effect of differential roughness on boundary shear stress distribution along the periphery of a symmetrical compound channel cross section as well as the flow distribution by varying the differential roughness in 4 ways.

➤ To study the velocity contours mapped from the experimental data taken at different points of the channel cross section grid for increasing differential roughness keeping the geometry (i.e. width ratio, slope) of the channel constant.

➤ To study the changing patterns in depth-averaged velocity with increasing relative depth as well as increase in differential roughness.

➤ To investigate the effect of differential roughness on the zonal Mannig's n during overbank flow and on the overall Manning's n for inbank as well as overbank flow.

➢ To study other previous methods of estimating percentage shear force carried by the floodplain in a compound channel flow with present experimental data as well as FCF data.

➢ Development of model to predict the percentage of shear force carried by floodplain for compound channels having high width ratio and rougher floodplain surface than the main channel and validation of the developed model with the data obtained through laboratory experiments and with the FCF data, which is used as benchmark in hydraulics research.

1.5   Organisation of the Thesis

The thesis comprises of six chapters.

Chapter-1 presents a brief introduction to channel's non-uniformity in roughness. The objective of the present investigation has been presented along with the relevant background information and gives an overview of the work undertaken for the research which is presented in the dissertation.

Chapter-2 presents literature review of the existing work of pioneer investigators. This chapter includes brief description of the research carried out in straight channel having smooth or rough surface; based on stage-discharge relationships, resistance coefficients, depth-average velocity, flow distribution and boundary shear distribution.

Chapter-3 describes experimental investigation, which include the experimental channel design, design and construction of roughness pattern, determination of base n value of the channel surface materials, notch calibration including experimental procedure of bed slope calculation, depth of flow and discharge measurement, and velocity measurement.

Chapter-4 include results concerning stage-discharge, stream-wise dimensionless velocity contour, boundary shear stress and boundary shear force along with theoretical considerations and description.

Chapter-5 includes the analysis of the results concerning depth averaged velocity, zonal and overall Manning's n variation, shear force distribution, modelling of shear force distribution method and validation test of the proposed model.

Chapter-6 presents the concluding remarks and outlines the scope of future work.

The works done by previous investigators, which are referred to in the subsequent chapters, have been cited at end of the dissertation in the reference section.

Chapter 2

REVIEW Of LITERATURE

2   REVIEW OF LITERATURE

Flow characteristics, like boundary shear distribution, flow distribution, depth-averaged velocity, and flow resistance, etc., have been studied by many investigators since last eight decades. This chapter presents some of the compound channel studies that motivated and inspired this dissertation research.

2.1   Studies in Smooth Compound Channels

Sellin (1964) was the first to investigate the momentum transfer mechanism in a compound channel, which was manifested by a series of vortices having vertical axis, along the interface of main channel and floodplain and presented photographic evidence of the presence of vortices at the interface of main channel and floodplain. He studied the channel velocities and discharge under both interacting and isolated conditions. Under isolated condition, the velocity in the main channel was observed to be more than that in the interacting condition.

Zheleznyakov (1971) confirmed the presence of momentum transfer mechanism between the main channel and the adjoining floodplain. The relative 'drag' and 'pull' between the faster moving main channel flow and slower moving floodplain flow gave rise to the momentum transfer mechanism, which he named "kinematics effect". He carried out laboratory investigation to study the effect of momentum transfer mechanism, which was responsible for decreasing the overall rate of discharge for floodplain depths just above the bank full level. As the floodplain depth increased, the importance of the phenomena diminished. He also carried out field experiments to confirm the significance of the momentum transfer phenomenon in the calculation of overall discharge.

Myers and Elsawy (1975) studied the flow interaction phenomenon and quantified the impact of lateral momentum transfer on the main channel flow velocity, discharge and the distribution of boundary shear stress for non-interacting (isolated floodplain flow) and interacting condition (combined main channel and floodplain flow) in a straight asymmetric compound channel section (one sided floodplain). They compared the observed boundary shear stress distributions obtained under interacting and non-interacting conditions and found that maximum shear stress of floodplain increases 260% for their shallowest floodplain depth. The understanding of the mechanism of local scour and estimation of maximum scour for floodplain zones in such circumstances is

dependent on the understanding of the lateral momentum transfer and proper account of it respectively.

Rajaratnam and Ahmadi (1979) studied the flow interaction effect in a straight compound channel having smooth symmetrical floodplains. They demonstrated the momentum transfer from main channel to floodplain during overbank flow condition. Due to flow interaction, the bed shear in floodplain - main channel interface increased considerably and that in the main channel decreased. They also observed that the reduction of the flow interaction effect increased with the increment of the flow depth on the floodplain.

Knight and Demetriou (1983) carried out laboratory investigation in straight compound channels with symmetrical floodplains to study the discharge characteristics; boundary shear stress and boundary shear force distributions in the compound section. They proposed equations for estimating the percentage of shear force carried by floodplain and also the proportions of total flow in various sub-areas of compound section in terms of two dimensionless channel parameters. On account of interaction of flow between floodplain and main channel, it was observed that the division of flow between the subareas of the compound channel did not follow the simple linear proportion to their respective areas.

Wormleaton and Hadjipanos (1985) studied flow distribution in compound channels. They concluded that even though a calculation method may give satisfactory results of overall discharge in a compound channel at greater floodplain depth with smoother floodplains, the distribution of flow between floodplain and main channel may be insufficiently modelled which leads to very erroneous values due to momentum and kinetic energy flux.

Myers (1987) proposed theoretical considerations of ratios of main channel velocity and discharge to the floodplain values in compound channel. These ratios were found to be independent of bed slope but dependent on the channel geometry. These ratios established a straight line relationship with the depth flow. The relationships were presented in terms of mathematical equations for smooth symmetrical compound channel. From the observations it was concluded that at low depths, the conventional approach of discharge estimation always overestimate the carrying capacity of the full cross section and underestimated at large depths, while floodplain flow capacity was always

underestimated at all depths. He pointed out the need for accurate modelling of flow distribution in floodplain and main channel as well as the discharge capacity of the compound channel cross-section as a whole.

Myers and Brennan (1990) analysed first series results of FCF (Flood Channel Facility) data to assess flow resistance characteristics of simple and compound channels having smooth boundaries. They studied the effect of momentum transfer from main channel to floodplain on the discharge carrying capacity of both the main channel and floodplain. They presented flow resistance relationship for the main channel and floodplain in terms of Manning's and Darcy-Weisbach roughness coefficients. They opined that the simple channel method of analysis and design is not appropriate for rivers and compound channels.

Lambert and Myers (1998) proposed a method for predicting the stage-discharge relationship in a straight compound channel. The proposed method developed from an investigation of the changes in the mean velocity of the main channel and the floodplain regions due to the momentum interaction between the regions. They used FCF experimental results to develop a method which was capable of more accurately representing the component mean velocities, which results in improved estimation of both zonal and the overall discharge values.

Al-Khatib and Dmadi (1999) studied boundary shear stress distribution in a straight symmetrical rectangular compound channel comprising rectangular main channel. They presented the relation of different dimensionless ratios of shear stress distributions with relevant parameter of flow like discharge, relative depth and floodplain depth.

Atabay and Knight (2002) presented equations of stage discharge relationship for symmetrical compound channel section using the Flood Channel Facility (FCF) data. They investigated the influence of floodplain width and main channel aspect ratio on the stage discharge relationship. They proposed simple empirical relationships of stage discharge with total discharge as well as zonal discharge for uniform roughness and varying floodplain width ratio. They also studied the effect of floodplain width ratio on the stage-discharge relationship.

Abaza and Al-Khatib (2003) conducted experimental testing of five different types of boundary shear stress distribution, viz., average shear stress at the bottom of the main

channel, average shear stress at the bed of flood plain, maximum shear stress at the bottom of the main channel, maximum shear stress at the bed of flood plain and shear stress at the bottom of main channel centreline, in six types of symmetrical rectangular compound channels. They derived a generalized multiple-variable regression model to predict each of the five experimentally measured shear stresses as a function of three dimensionless parameters. They also presented a single multi-variable regression model for estimating mean shear stress at the bottom of a rectangular compound cross-section using average values of obtained regression coefficients of the multiple-variable regression model.

Hosseini (2004) studied discharge characteristics in straight compound channels having homogeneous roughness by acquiring a large body of experimental data which covered small scale and large scale laboratory compound channels. He proposed a method for discharge calculation in these channels by analysing some experimental results from FCF. The proposed method used two correction coefficients, which were applied to the component mean velocities predicted by the traditional vertical division method in order to find more accurate values of the mean velocities in the main channel and floodplains. He expressed the coefficients in terms of two dimensionless parameters of the channel, coherence and the relative depth, viz., ratio of the floodplain depth to the total depth.

Knight et al. (2010) proposed a simple lateral distribution model based on the Shiono & Knight method (SKM), which is useful for analyzing a range of practical problems in river engineering. They also demonstrated the usefulness of the model in predicting lateral distributions of boundary shear stress and depth-averaged velocity, stage-discharge relationships, as well as indicating how to deal with some sediment and vegetation issues.

Rezaei and Knight (2011) presented experimental results of overbank flow in compound channels with nonprismatic floodplains and different convergence angles. They measured depth-averaged velocity, local velocity distributions and boundary shear stress distributions along the converging flume portion for different relative depth flow. They used the momentum balance to analyze the force acting on the flow in the main channel and for the whole cross section. They estimated the apparent shear forces on the vertical interface between the main channel and floodplains for compound channels

having nonprismatic floodplains then compared the obtained value with the prismatic cases.

Khatua et al. (2012) presented a modified equation to estimate boundary shear distribution in compound channels. They proposed a method to predict the stage-discharge relationship using one-dimensional approach. The proposed method was established by taking the momentum transfer into account. The presented method was tested for natural channels and found to give satisfactory results.

2.2   Studies in Rough Compound Channels

Ghosh and Jena (1973) studied boundary shear distribution in straight compound channels for both smooth and rough boundaries. They correlated the contribution of the total drag force exerted by different segments of the channel section to the flow depth of and roughness concentration.

Knight and Hamed (1984) extended the work of Knight and Demetriou (1983), to the compound channels having rough floodplains. By adding strip roughness elements at specific longitudinal spacing, the floodplains were roughened in six different ways. They studied the influence of differential roughness between floodplain and main channel on the process of lateral momentum transfer. They presented equations for estimating the percentage of shear force carried by floodplains of total shear force in a compound channel flow by using dimensionless channel parameters (e.g. the width ratio, depth ratio, roughness ratio, and aspect ratio). They also investigated the discharge distribution for the same compound channel.

Myers and Lyness (1997) studied the behavior of two key discharge ratios, namely total to bank full discharge and main channel to floodplain discharge in compound channels for smooth and homogeneously roughened channels of various scales by the help of acquired data of small-scale and large-scale laboratory compound channels as well as natural rivers. The total to bank full discharge ratio was found to be independent of bed slope and scale but a function of cross section geometry only. The other ratio, i.e. the main channel to floodplain discharge was also independent of bed slope and scale but was influenced by the lateral floodplain bed slope. They evaluated the coefficients and exponents in the equations relating to flow ratios to flow depths.

Myers et al. (2001) presented of an experimental results of a compound channel having fixed and mobile main channel along with two rough floodplains. They investigated velocity and discharge relationships illustrating the complex behaviour of compound channel river section. They underlined the error incurred in applying conventional methodologies to discharge assessment in overbank flow conditions. They presented relationships for velocity and discharge which could form the base of mathematical modelling of overbank flow estimation methods.

Seckin (2004) investigated the reliability and performance of four different one-dimensional methods of computing the discharge capacity for compound channels by conducting a series of experiments in a compound channel having a smooth main channel and smooth or rough floodplains. For the study, he roughened the floodplains in four different ways using metal meshes. The metal meshes had a width of 35.5cm, a height of 14.5cm and an angle of 30° and were placed at 4 different intervals spacing on each floodplain in order to provide a particular roughness. A separate series of experiments were undertaken to find out their exact resistance properties of floodplain roughness were created.

Hin and Bessaih (2004) investigated velocity distribution, stage-discharge relationship and the effect of momentum transfer in a straight compound channel having a rougher floodplain than the main channel. They artificially roughened the floodplain by using wire mesh.

Yang et al. (2005) presented the relationships between the local, zonal and overall resistance coefficients (Manning's *n* and Darcy-Weisbach's *f*) for a wide range of variation in channel geometries and different roughness between the main channel and the floodplain by using FCF (Flood Channel Facility) data. They pointed out that the functional relationship of Darcy-Weisbach resistance coefficient with Reynolds number in a single channel is different from that in a compound channel. They also found that the local resistance coefficients approximately remain constant for a certain given relative depth, but are different in the main channels and on the floodplains in smooth compound channels; however in case of a roughened compound channel and an asymmetric one, these coefficients decrease as the relative depth increases.

Yang et al. (2007) studied the resistance characteristics of inbank and overbank flows by conducting a series of experiments in a large symmetric compound channel

having a rough main channel and rough floodplains. They analyzed the effective resistance coefficients (i.e. Manning's *n*, Darcy–Weisbach's *f,* Chezy's C) and the relative Nikuradse roughness height and concluded that these flow resistance coefficients vary with the flow depth in a complicated way for the overbank flow in the large compound channels with a rough bed. They validated many methods of predicting the composite roughness using the laboratory data and collected field data for compound channels. They analyzed the errors obtained during validation test and gave proper reasons for those errors.

Joo and Seng (2008) compared the different methods available for discharge prediction in a compound channel. They carried out experimental investigations on a small scale non-symmetrical compound channel with rough flood plain. They used the weighted divided channel method to check the validity of the horizontal division method and the vertical division method in predicting discharge. They underlined that the horizontal division method provide more accurate predictions of discharge for non-symmetrical compound channel with wider flood plain, while the vertical division is more accurate for narrower flood plain.

Kean et al. (2009) investigated velocity and boundary shear stress distributions across the cross-section of a straight compound channel whose floodplain was roughened by cobble. They presented a method of estimating boundary shear and velocity taking the drag force on clasts found in the channel. They pointed out that the principal differences between the measured and calculated fields were the results of secondary circulations, which were not taken into account for the calculation. By varying the width of the channel, they studied the effect of the width-to-depth ratio on the velocity and boundary shear stress across the channel.

Chapter 3

EXPERIMENTAL INVESTIGATION

3 EXPERIMENTAL INVESTIGATION

In order to find out the effect of diversity in floodplain roughness and main channel roughness on the flow characteristics (i.e. boundary shear distribution, flow distribution, depth-averaged velocity, variation in overall and zonal Manning's n and discharge) during over flow condition in a compound channel, experiments were conducted under controlled laboratory conditions in the Fluid Mechanics and Hydraulics Laboratory of the Civil Engineering Department at the National Institute of Technology, Rourkela, India. Experiments were conducted in the channel by changing the roughness of the floodplain with respect to the main channel. This chapter describes the experimental channel design, roughness elements design and determination of base n value for the roughness elements used.

3.1 Experimental Channel Design

3.1.1 Tilting Flume

For the present study a straight compound channel was used, which was fabricated inside a tilting flume having dimension 12m long, 2m wide and 0.6m depth. At the beginning of the flume just after inlet and before head gate (called stilling chamber), a series of baffle walls were installed for energy dissipation purpose, i.e. to reduce turbulence and make water body still before passing over the channel. Head-gate reduces the waves if formed in the water body before it passes over the channel and in this way head-gate plays a vital role in having uniform flow. Travelling bridges were there to carry measuring instruments. Tailgate was provided just before end point of the flume for bed slope measurement purpose. Rectangular notch was installed at the end of the flume to measure discharge for each run. Over bridge platform was there, which made experimental work easy over 2m wide flume. A bell-mouth entrance was attached to the experimental channel to ensure that the flow is uniform over the intake section and the head loss induced at inlet section is minimized. The sketch of whole system with plan view of the tilting flume with experimental channel (not to scale) is shown in Fig. 3.1. The flume was supported on a hinge at the centre and made tilting by providing hydraulic jack arrangement at starting point of the flume.

14
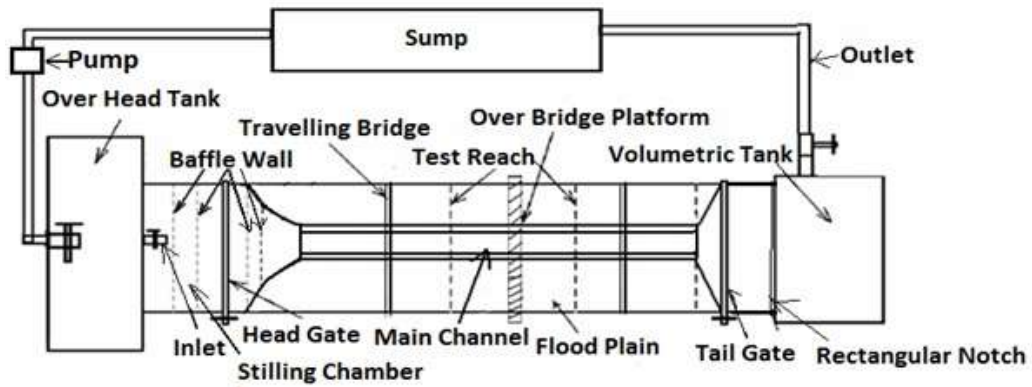
Fig. 3.1 Schematic drawing of whole experimental system with tilting flume

3.1.2 *Experimental Compound Channel*

The compound channel used for investigation comprised a main trapezoidal channel of 120 mm wide at bottom, 280 mm wide at top having depth of 80 mm and side slopes of 1:1 along with symmetric floodplains of 805mm width, 120mm height and zero side slope, on both sides of the main channel (Fig. 3.2). The whole channel was fabricated by using 5mm thick Perspex sheets. Detailed geometrical features of the experimental channel are given in Table 1.
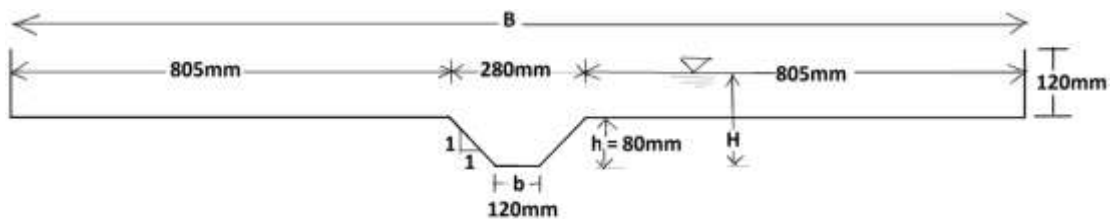
Fig. 3.2 Cross sectional view of the experimental channel

Table 1. Detailed Geometrical Features of The Experimental Channel

Sl no.	Item description	Current Experimental Channel
1	Channel type	Straight
2	Geometry of main channel section	Trapezoidal (Side slope1:1)
3	Geometry of floodplain section	Rectangular (Side slope 0)
4	Floodplain type	Symmetric
5	Main channel base width (*b*)	0.12m
6	Top width of Compound channel (*B*)	1.89m
7	Depth of main channel (*h*)	0.08m
8	Bed slope of the channel	0.00311
9	Width ratio ($\alpha = B/b$)	15.75
10	Aspect ratio ($\delta = b/h$)	1.5

3.1.3   Water Supply System

Water for the experiment was supplied from an overhead tank to which a water level indicator was attached to maintain constant water level in the overhead tank. Two parallel pumps were installed for pumping water from an underground sump to the overhead tank. Water delivered to the stilling chamber from the overhead tank, passed over the experimental channel under gravity and was allowed to flow over rectangular notch before falling to a volumetric tank situated at end of the flume. From the volumetric tank it was allowed to flow back to an underground sump. From the sump water was pumped back to the overhead tank for recirculation. The circulating water supply system is shown in Fig. 3.3.
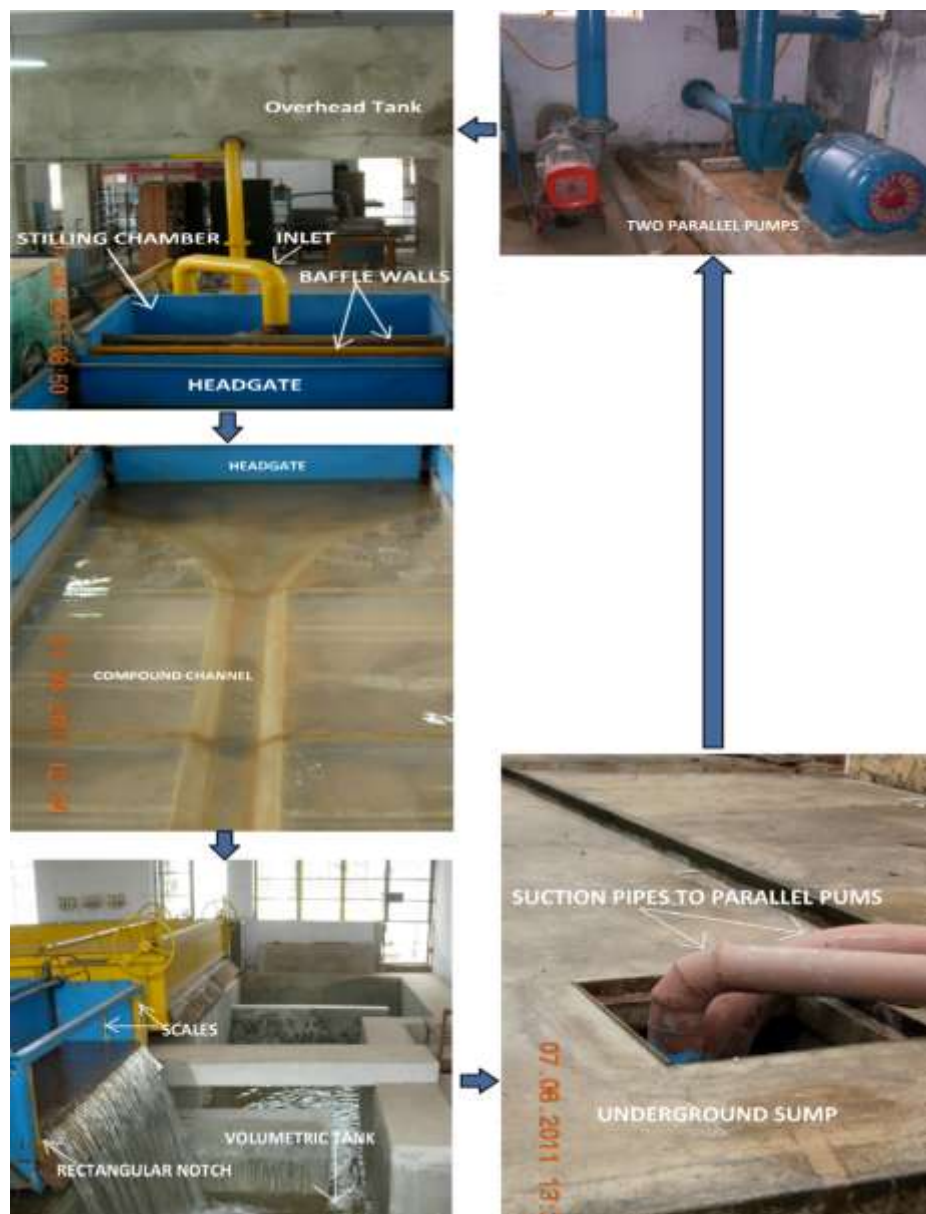
Fig. 3.3 Water supply system

3.2 Notch Calibration

The volumetric tank was reconstructed in the Fluid Mechanics Laboratory and a rectangular notch of 1.86m length and 0.1m height was newly installed at the end of the experimental flume for accurate discharge measurement of each run. For discharge measurement, the rectangular notch needed calibration. The area of the volumetric tank was measured properly thrice and average of it was found out to be 20.928784m^2. Height of water in volumetric tank was monitored in a glass tube water level indicator attached to it. The discharge into the volumetric tank was measured by the time to rise method. The change in the depth of water in the volumetric tank with time was measured with the help of a stopwatch having accuracy of 0.01 sec. The height of water flow above the notch was measured with the help of the scale attached to it. The coefficient of discharge (C_d) of the rectangular notch was found out by calibrating the rectangular notch with the actual discharge in the volumetric tank. For this calibration the following formula were considered (Modi and Seth, 1998)

$$Q_a = C_d Q_t \tag{1}$$

$$Log Q_a = Log C_d + Log Q_t \tag{2}$$

where $Q_a = A_{vt} h_w$ and $Q_t = \frac{2}{3} L \sqrt{2g} H_n^{2/3}$ $\qquad$ (3)

where Q_a is the actual discharge, Q_t is the theoretical discharge, A_{vt} is the area of the volumetric tank, h_w is the height of water in the volumetric tank, L is the length of the notch, H_n is the height of water flow above the rectangular notch, and g is the gravitational acceleration. A graph between $Log Q_t$ and $Log Q_a$ was plotted (shown in Fig. 3.4). From the graph, $Log Q_a$ was found to be linearly dependent on $Log Q_t$ and the intercept value was taken as the $Log C_d$ value as per Eq. (2). From the intercept value, the C_d value of the notch was found out to be 0.6792 (for the particular slope of the channel mentioned in section 3.5.1). Photograph of the rectangular notch calibration experiment is shown in Fig. 3.5.
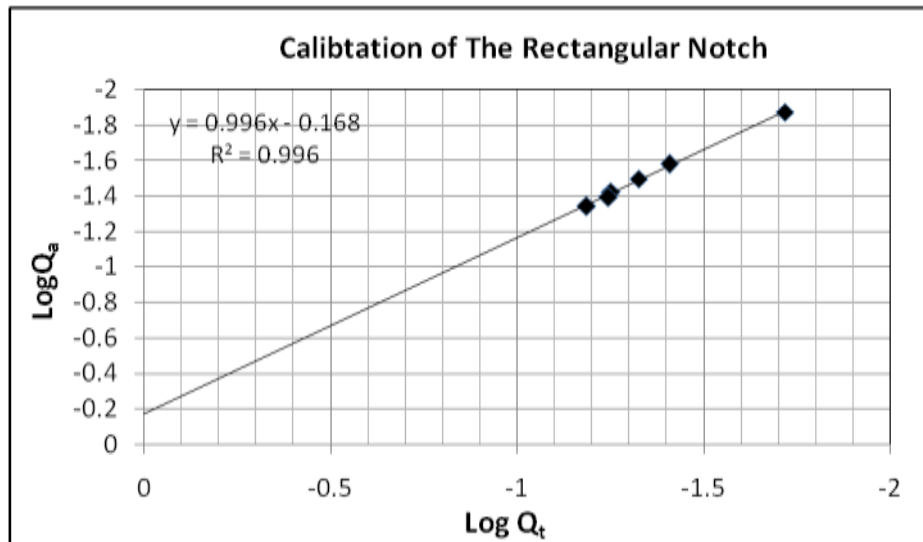
Fig. 3.4 Calibration chart of the rectangular notch

Fig. 3.5 Rectangular-Notch calibration experiment

3.3 Design and Construction of Roughness Patterns

The compound channel boundary was roughened by using two types of roughening material across the channel cross section. Based on previous investigations concerning rough channel surface (Alhamid, 1991; Seckin, 2004; Hin and Bessaih, 2004; Maghrebi and Rahimpour, 2006; Joo and Seng, 2008; Blanckaert et al., 2010), woven wire mesh and crushed stone were used on the compound channel surface in order to have rougher floodplain than the main channel for this study.

3.3.1 Properties of Roughening Materials

Woven wire mesh having mesh opening size 3mm x 3mm was used as one of the roughening material in the present study. Its wire diameter was measured to be 0.4mm (Fig. 3.6).

Fig. 3.6 Woven wire mesh   **Fig. 3.7 Crushed stone**

Crushed stone was the other roughening material used in the present study (Figure 3.7). Before the channel roughening work, some of the properties of the crushed stone were found out. Specific gravity (S_g) of the crushed stone was calculated as per the procedure in IS: 2386 Part III [vi]. The angularity number of the stone was calculated following the procedure in IS: 2386 Part I [v] and the formula was:

$$\text{Angularity number (AN)} = 67 - \frac{100W_a}{S_g W_w} \qquad (4)$$

where W_a is the mean weight (in g) of the aggregate in the cylinder, W_w is the weight of water (in g) required to fill the cylinder, and S_g is the specific gravity of aggregate. As per IS: 1607 [vii] sieve analysis was done for the stone to find out its particle size distribution. The percent finer range for the stone is shown in Fig. 3.8. The equivalent sand roughness (k_s) value, the coefficient of gradation (C_g), the coefficient of uniformity (C_u), the geometric standard deviation (G_s) and the geometric mean diameter (D_g) of the stone, were obtained from the particle size distribution graph (mentioned in Table 2) are defined as (Rice et al. (1998), Patel and Ranga Raju (1999)):

$$k_s = d_{50}, C_g = \frac{d_{30}^2}{d_{60}d_{10}}, \ C_u = \frac{d_{60}}{d_{10}}, \ G_s = \frac{d_{50}}{d_{84}} \ \text{and} \ \log D_g = \frac{\sum(\Delta p_i \log di)}{100} \ (5)$$

Table 2. Properties of The Stone (Roughening-material)

Equivalent Sand Roughness (k_s) in mm	3.39
Coefficient of Gradation (C_g)	0.78346
Coefficient of Uniformity (C_u)	1.816832
Geometric Standard Deviation (G_s)	1.262537
Geometric Mean Diameter (D_g)	2.65
Specific Gravity (S_g)	2.68
Angularity Number (AN)	11
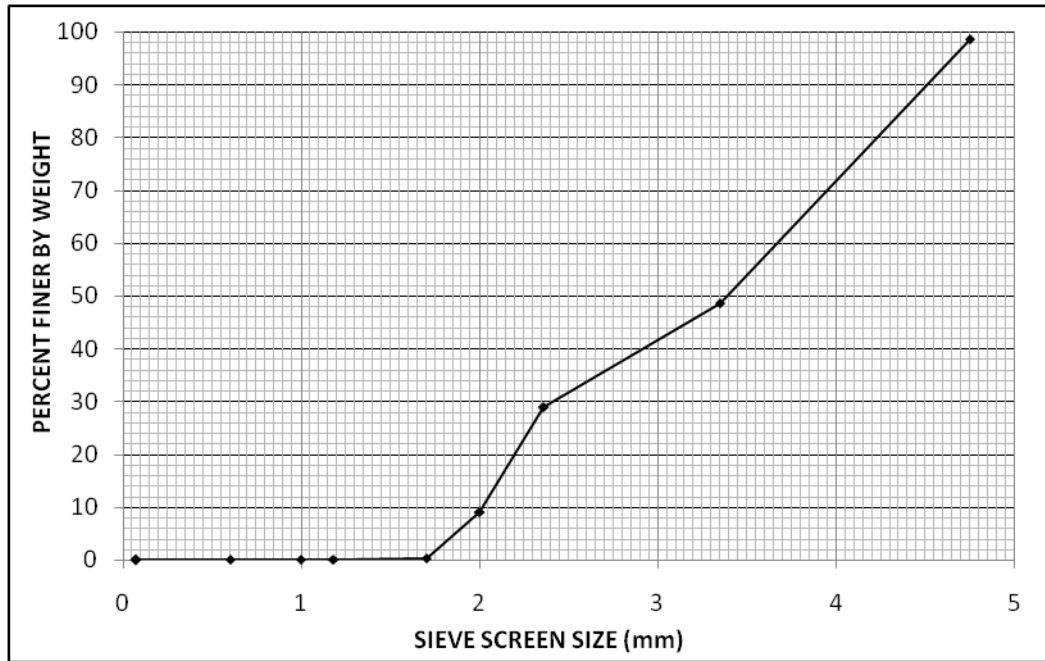
Fig. 3.8 Particle size distribution of stone-roughness material

3.3.2 Determination of base n value of channel surface materials

Roughness of a material is generally expressed in terms of roughness coefficient which gives resistance to flow. In usual practice of one dimensional flow analysis, the selection of an appropriate value of roughness coefficient is needed for evaluating the carrying capacity of a channel. The experimental results of FCF, phase-A, indicate that the variations of the Manning's *n* with the flow depth are different for the inbank and overbank flows. With the increasing flow depth, Manning's *n* returns to the more common value which shows that the Manning's *n* is a function of the flow depth at a low flow depth for the overbank flows. Composite roughness also varies with depth of flow. To avoid this complexity, inbank flow experiments were conducted to obtain the base *n* (Manning's *n*) value of the perspex sheet, wire mesh and stone. The mean values of resistance coefficient (*n*) from the inbank flow experiments were adopted as respective material's resistance coefficient for overbank flow conditions in the present study. This procedure of Manning's *n* determination of a material has been adopted based on the study of many previous investigators, Myers and Brennan (1990), Ayyoubzadeh (1997), Atabay and Knight (2006), Atabey's Birmingham data [i] and Tang's Birmingham data [ii]. The Mannig's formula (Chow, 1959), was used for determination of the base *n* value of these materials.

$$n = \frac{1}{U} R^{2/3} S^{1/2} \tag{6}$$

where *U* is the mean velocity in the channel, *R* is the haydraulic radius (*A/P*) where *A* is the area of flow and *P* is the wetted perimeter of the cross-section, and *S* is the energy gradient slope.

The materials used in the construction of creating various roughness patterns in the compound channel were perspex sheet, woven wire mesh and crushed-stone roughness (the same mentioned above). For determination of base *n* value of these materials, three series of experiments were performed in inbank flow condition.

For inbank flow experiments, the mesh and stone were applied to the test reach area phase by phase. The test reach length was 42.85% of the compound channel length (i.e. 3m of the 7m compound channel) taken at 3m from the end of point of the bell-mouth section. First series was in smooth condition i.e. flow in main channel which was made up of perspex sheet (already available). Second series was conducted putting the woven wire mesh in main channel boundary. Third series was conducted in main channel, whose boundary was covered with the stone roughness element. The construction of mesh roughened and stone roughened main channel are given below.

3.3.2.1 *Construction of Mesh Roughened Main Channel*

To create mesh roughened main channel the subsequent steps were followed. Step 1: The woven wire mesh was laid on a plain surface and was rolled properly to make it straight. Step 2: It was cut in to pieces of total length of the main channel cross section at test reach. Step 3: Then these pieces were given main channel cross section shape. Step 4: At last these pieces were glued to the main channel by using adhesive and left for 24hrs to dry before experimentation work. By this process, the surface area of the main channel of the test reach was roughened. The schematic drawing of the mesh roughened main channel cross-section is shown in Fig. 3.9 and the making of the mesh roughened main channel is shown in Fig. 3.10.

Fig. 3.9 Schematic drawing of the mesh roughened main channel cross-section

Fig. 3.10 Construction of mesh roughened main channel

3.3.2.2 *Construction of Stone Roughened Main Channel*

To create stone roughened main channel the subsequent procedure was adopted. Step 1: Stone material was glued to the main channel by using adhesive and left for 24hrs to dry. Step 2: After 24hrs, the excess material was swept out to get uniform roughness in the channel. Like this, stone roughening material was applied to the main channel of the test reach section. The schematic drawing of the stone roughened main channel cross-section is shown in Fig. 3.11 and the construction of the stone roughened main channel is shown in Fig. 3.12.

Fig. 3.11 Schematic drawing of the stone roughened main channel cross-section

Fig. 3.12 Constriction of stone roughened main channel

3.3.2.3 *Experimentation for base n value*

For determination of base *n* value of the perspex sheet, wire mesh and stone a series of inbank flow experiments were carried out. For stone roughened channel, the datum of the channel surface was considered at the height of geometric mean diameter of the stone. In each series discharge was found out for 5-7 depths of flow, from which velocity of the flow was calculated. Then by using the Manning's equation (Eq. 6), the *n* value was calculated for each run of inbank flow series. Then the mean of *n* in each series was taken as the base *n* value of the respective material, tabulated in Table 3 (as per discussion in section 3.3.2). These materials were further used in the experimental compound channel to create variety of roughness pattern for the present study. The photograph of inbank-flow experiments are shown in Fig. 3.13 (a,b,c).

Table 3. Base *n* Values of The Channel Surface Elements

Material	Flow depth, H (m)	Area of flow, A (m²)	Wetted Perimeter, P (m)	Hydraulic radius, R (m)	Discharge, Q (m³/s)	Velocity, U (m/s)	Slope, S x 10^3	Manning's *n*	Aver-aged *n*
Perspex sheet	0.059	0.0106	0.2869	0.0368	0.0072	0.6815	3.112	0.00906	0.00983
	0.064	0.0118	0.3010	0.0391	0.0077	0.6561	3.112	0.00980	
	0.066	0.0123	0.3067	0.0400	0.0081	0.6587	3.112	0.00991	
	0.070	0.0133	0.3180	0.0418	0.0086	0.6492	3.112	0.01035	
	0.075	0.0146	0.3321	0.0440	0.0102	0.6945	3.112	0.01002	
Wire Mesh	0.057	0.0101	0.2812	0.0359	0.0059	0.5799	3.112	0.01046	0.01097
	0.060	0.0108	0.2897	0.0373	0.0065	0.6030	3.112	0.01032	
	0.065	0.0120	0.3038	0.0396	0.0072	0.5986	3.112	0.01082	
	0.070	0.0133	0.3180	0.0418	0.0079	0.5944	3.112	0.01131	
	0.076	0.0148	0.3335	0.0443	0.0086	0.5850	3.112	0.01193	
Stone	0.056	0.0095	0.2727	0.0349	0.0040	0.4213	3.112	0.01415	0.01449
	0.059	0.0102	0.2812	0.0363	0.0043	0.4213	3.112	0.01452	
	0.064	0.0114	0.2953	0.0386	0.0049	0.4301	3.112	0.01482	
	0.068	0.0124	0.3066	0.0404	0.0055	0.4464	3.112	0.01471	
	0.070	0.0129	0.3123	0.0413	0.0059	0.4539	3.112	0.01468	
	0.073	0.0137	0.3208	0.0426	0.0065	0.4767	3.112	0.01427	
	0.075	0.0142	0.3264	0.0435	0.0069	0.4830	3.112	0.01428	

(a) Perspex sheet   (b) Wire mesh   (c) Stone

Fig. 3.13 Inbank flow experiments for determination of base *n* value

3.3.3   Construction of Rough Compound Channels

In overbank flow condition, four series of experiments were performed. First series of experiments were carried out in the compound channel having its entire surface smooth. For second series, floodplain bed and wall were roughened with the woven wire mesh keeping main channel surface smooth. In third series, main channel surface and floodplain wall were roughened with woven wire mesh where as the floodplain bed was uniformly roughened with the stone. Fourth series of experiments were performed in the compound channel having floodplain wall and main channel surface smooth along with the stone roughened floodplain bed. Boundary conditions of overbank series are tabulated in Table 4.

Table 4. Channel Boundary Condition of all Overbank Flow Series

Series	Main Channel Boundary	Floodplain Bed	Floodplain Wall	Named	No. of Runs
1	Smooth	Smooth	Smooth	Smooth	7
2	Smooth	Mesh Rough	Mesh Rough	Roughness-I	6
3	Mesh Rough	Stone Rough	Mesh Rough	Roughness-II	6
4	Smooth	Stone Rough	Smooth	Roughness-III	6

3.3.3.1 Construction of Roughness -I

For construction of Roughness-I, Step 1: The woven wire mesh was rolled properly on a plain surface to make it straight. Step 2: The wire mesh was cut in two pieces of 3m length each. Step 3: Then these pieces were given floodplain cross section shape of the compound channel. Step 4: Lastly these pieces were glued to the floodplain bed and wall by using adhesive and left for 24hrs to dry before experimentation. The total floodplain surface of the test reach was roughened by this process. The schematic drawing of the Roughness-I and photograph of it are shown in Fig. 3.14 and Fig. 3.15 respectively.
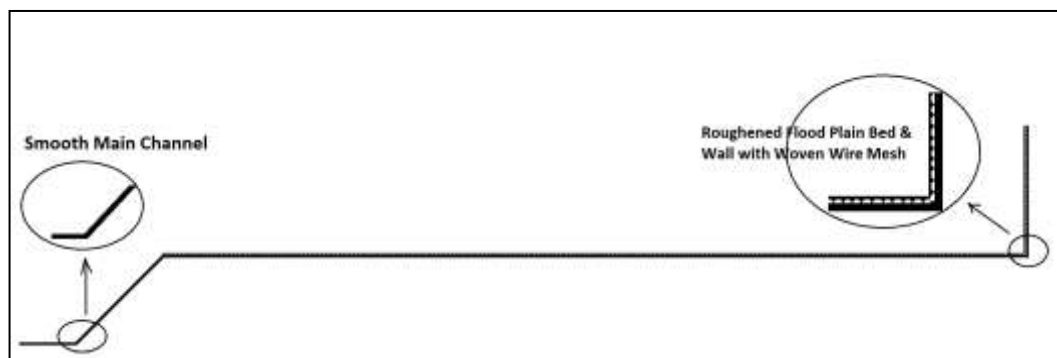
Fig. 3.14 Schematic drawing of Roughness-I
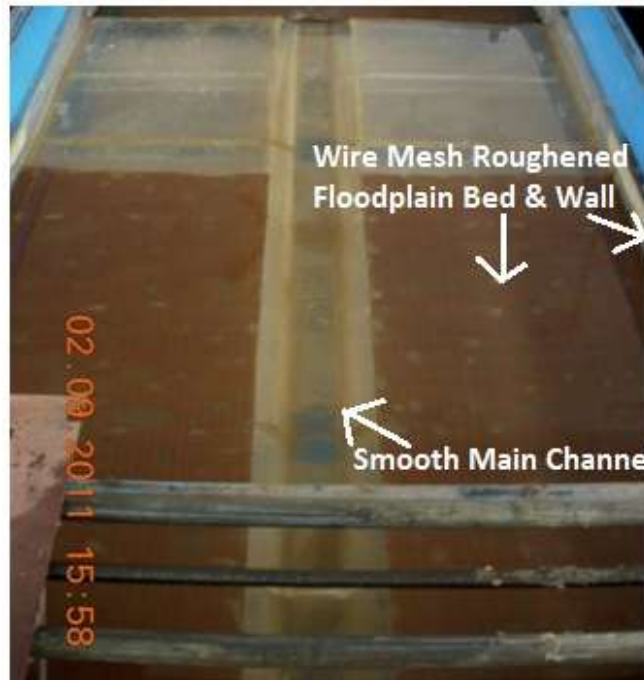
Fig. 3.15 Roughness-I

3.3.3.2 *Construction of Roughness-II*

Construction of Roughness-II, Step 1: Stone material was glued to the floodplains of the compound channel by using adhesive. Step 2: Then it was rolled to get uniform roughness and left for 24hrs to dry. Step 3: Excess stone material was swept out. This way both side floodplain beds of the test reach (3m length each) were roughened. Step 4: Mesh roughness, was put in main channel surface as it was done for inbank flow experiment and for floodplain wall roughness, wire mesh of Roughness-I was kept as it was. At last the compound channel with floodplain walls having mesh roughness, floodplain bed having stone roughness and main channel having mesh roughness was ready for the experiment. The schematic drawing of it is shown in Figure 3.16 and the construction of Roughness-II is shown in Figure 3.17.
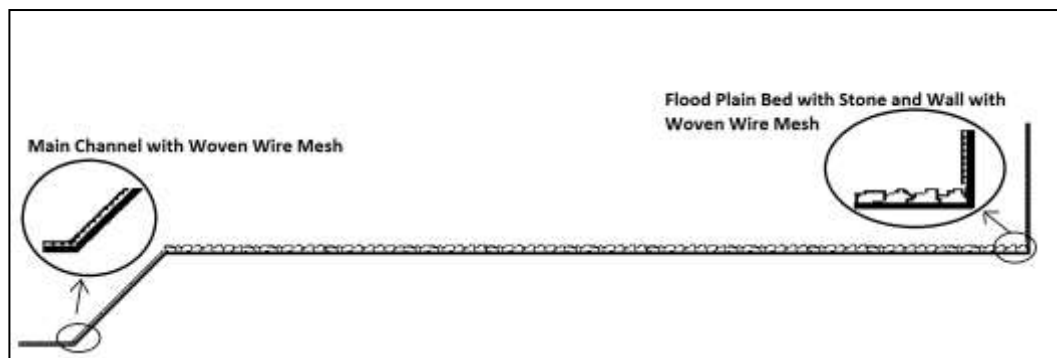
Fig. 3.16 Schematic drawing of Roughness-II

Fig. 3.17 Construction of Roughness-II

3.3.3.3 *Construction of Roughness-III*

For construction of Roughness-III, stone material roughness in Roughness-II was kept and the main channel surface and floodplain wall were made smooth by removing wire mesh. Further the leakage in main channel if any arise during removal of the mesh wire was repaired. The schematic drawing of Roughness-III and photograph of it, are shown in Figure 3.18 and Figure 3.19 respectively.
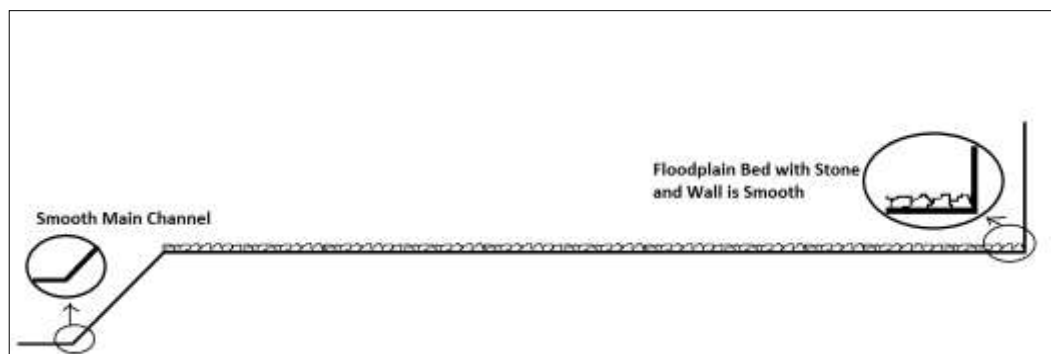
**Fig. 3.18 Schematic drawing of Roughness-III**

Fig. 3.19 Roughness-III

3.4 Determination of Differential Roughness (γ) value

In a river section, differential roughness in main channel and floodplain generally exists. River engineers usually use base *n* value of river subsections (as given in Chow (1959)) to calculate the flow and other parameters in a river section. The differential roughness "γ" is an important non dimensional parameter required to be found out for estimation of flow distribution, boundary shear distribution etc. (Knight and Hamed, (1984)). In this research, for every overbank experiment, the differential roughness (i.e. n_{fp} / n_{mc}) was changed, keeping floodplain bed rougher than the main channel as explained before. Due to some practical problem it was not possible to get uniformly roughened floodplain boundary. For all overbank series, the wetted perimeter of floodplain walls was less than 3% of the total wetted perimeter so that the effect of roughness of the floodplain walls could be neglected and only bed roughness of the floodplains to be taken into account. Using the base *n* value obtained from inbank flow experiments (in section 3.3.2.3), all the overbank flow series has been categorized in terms of "γ" (Table 5).

Table 5. Differential Roughness Value of all Overbank Flow Series

Series	Main Channel *n* (n_{mc})	Floodplain *n* (n_{fp})	Differential Roughness, γ (n_{fp}/n_{mc})
Smooth	Smooth	Smooth	1
Roughness-I	Smooth	Mesh Rough	1.12
Roughness-II	Mesh Rough	Stone Rough	1.32
Roughness-III	Smooth	Stone Rough	1.47

3.5   Experimental Procedure

Main parameters to be measured during the experiment were the discharge, bed slope and the velocity. Those were measured in the following procedure.

3.5.1   Calculation of Bed Slope

To find out the channel bed slope, the tailgate of the flume was closed. The main channel was pounded with water. The depth of water at two end points along the centreline of 3m long test reach was measured with the help of a point gauge having least count of 0.1mm. The point gauge was attached to the travelling bridge for which the point gauge was able to move in transverse as well as in longitudinal direction of the channel. The slope of the bed was found out by dividing the difference in depth of water at two ends of the test reach by the test reach length. From the measurement, the bed slope was found out 0.003112 and was kept constant for all inbank and overbank series of experiments.

3.5.2   Depth of Water and Discharge Measurement

Depth of flow for all inbank series and overbank series at the test reach section was measured with the help of point gauge. The height of flow above the notch for each run was also noted down for discharge calculation. The discharge (Q_a) for each run was calculated from the equation given below:

$$Q_a = C_d \frac{2}{3} L \sqrt{2g} H_n^{2/3} \tag{7}$$

where C_d is the coefficient of discharge of the notch calculated from calibration, L is the length of the notch, H_n is the height of water flow above the notch, and g is the gravitational acceleration.

3.5.3   Measurement of Velocity

A micro-pitot tube 6.33mm external diameter in conjunction with a suitable inclined manometer (inclined at 24.86^o with the horizontal) was used to measure velocity. The pitot tube was fixed to a main scale having vernier scale with least count 0.1mm. The main hole of the pitot tube was faced to the flow direction to give total pressure while the surface holes of the pitot tube gives static pressure. Both the pressures were seen as height of waters in two limbs of inclined manometer. The difference in water elevation gives the velocity at the particular point (U_p) where the pitot tube was mounted and also the pressure difference (Δp) by using the following Bernoulli equations (White, 1999).

The pressure difference (Δp) measured at different points on the wetted perimeter was further used for boundary shear calculation by preston tube technique (Section 4.3.2).

$$U_p = \sqrt{2g\Delta h \sin\theta} \tag{8}$$

$$\Delta p = \rho g \Delta h \sin\theta \tag{9}$$

where g is the gravitational acceleration, ρ is the density of water, Δh is the difference in water elevation in the manometer, θ is the angle of manometer with horizontal base. The measurement setup is shown in Fig. 3.20 and all overbank series experiments are shown in Fig.3.21 - 3.24.
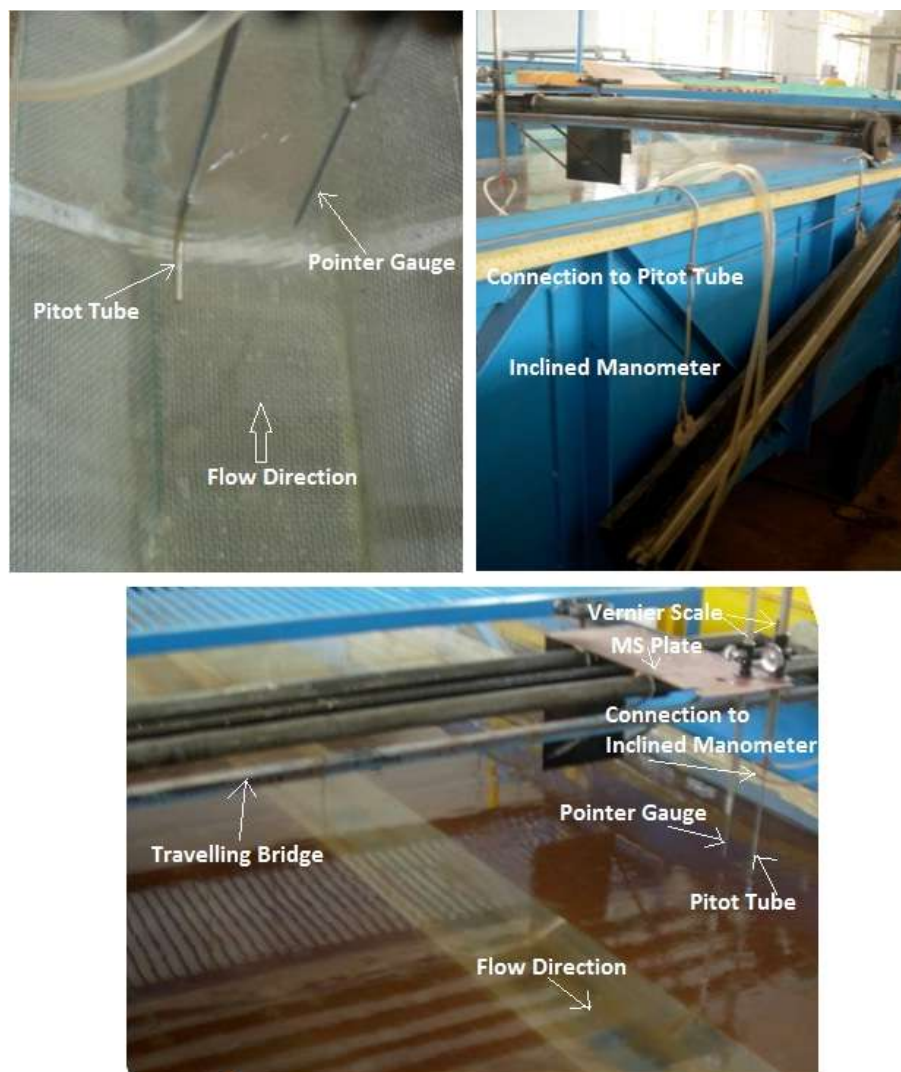
Fig. 3.20 Measurement setup

Fig. 3.21 Photograph of Smooth series experiment

Fig. 3.22 Photograph of Roughness-I series experiment

Fig. 3.23 Photograph of Roughness-II series experiment

Fig. 3.24 Photograph of Roughness-III series experiment

Chapter 4

EXPERIMENTAL RESULTS

4 EXPERIMENTAL RESULTS

The results of all the series of experiments conducted in this research are presented in this section. Variation in stage-discharge relationship and distribution of stream-wise velocity due to variation in differential roughness or roughness ratio (γ = the ratio of base *n* value of the floodplain surface material (n_{fp}) to that of the main channel (n_{mc})) are discussed in this chapter. Boundary shear evaluation technique, boundary shear stress and boundary shear force results are also included in this chapter.

4.1 Stage-Discharge Relationship

For the present investigation an overall steady and uniform flow during experimentation was maintained. To ease the analysis process, flow in all series was assumed to be steady and uniform; and hence the measured bed slope of the compound channel (section 3.5.1) was assumed to be the water surface slope. The slope was kept constant for all series of experiments in the present study. The depth of flow on main channel (*H*) was taken as the stage, which gave a particular discharge (Q_a) only under steady and uniform conditions. From the depth of flow over the rectangular notch, the actual discharge (Q_a) was found out by using Eq. (7) for each run of all series experiments. The stage vs. discharge curves for all series of overbank flow are plotted in Fig. 4.1, where we can see the variation in Stage-Discharge relationship with variation in differential roughness (γ) for the compound channels having constant geometry (i.e. width ratio ($\alpha = B/b$) and slope). In the Fig. 4.1, we can observe that:

- With the increase in depth of flow on main channel, discharge increases.

- For a constant depth of flow, discharge decreases with the increase in differential roughness (γ).

- Discharge of $\gamma = 1.12$, gradually becomes closer to $\gamma = 1$ as depth of flow increases, i.e. the roughness effect on flow decreases slowly with increase in depth of flow.

- For lower depths of flow, discharges of $\gamma = 1.32$ and $\gamma = 1.47$ are found nearly equal, where as discharge of $\gamma = 1.47$ becomes more than of $\gamma = 1.32$ as depth of flow increases. Which may be due to the roughness effect of main channel

increases with the increase in depth of flow for $\gamma = 1.32$ (as the main channel is mesh roughened in case of $\gamma = 1.32$ while it is smooth in case of $\gamma = 1.47$).
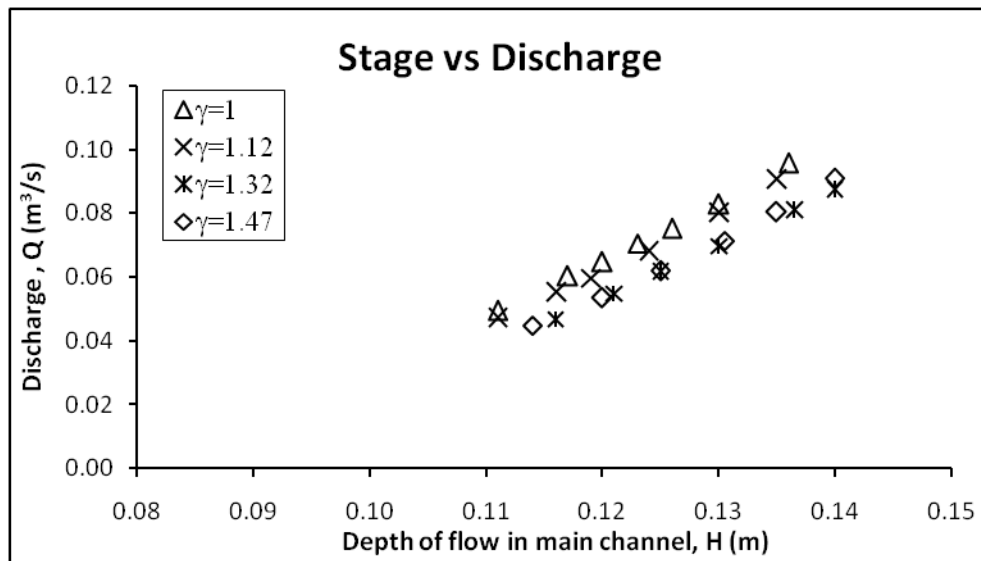
Fig. 4.1 Stage-Discharge relationship for compound channels with different roughness ratio

4.2 Distribution of Stream-wise Velocity

In the present work, the stream-wise velocity at all points (U_p) of the grid of the flowing cross section, were found out by using the pitot tube for each run of all overbank series flow. As the compound channel was symmetric, only half of the channel was considered for the measurement of stream-wise velocity. For mapping of contours, the middle of the main channel is taken as origin and the base as datum. The distribution of dimensionless stream-wise velocity (U_p/U) in contour form for Smooth, Roughness-I, Roughness-II and Roughness-III series are shown in Fig.4.2, Fig.4.3, Fig.4.4 and Fig.4.5 series respectively (where U is the mean velocity of a run).

From the observation of dimensionless stream-wise velocity isovels of contours for the Smooth series (i.e. $\gamma = 1$), shown in Fig. 4.2.1-4.2.7, the following conclusions can be drawn.

- The velocity variation on floodplain gradually becomes stabilised with the increase in depth of flow.

- The concentration of higher velocity contours on the floodplain increases with the increase in depth of flow which shows that the velocity on the floodplain increases

with the increase in depth of flow (i.e. the percentage of flow on the floodplain increases with increase in flow).

- The concentration of lower velocity contour isovels increases in main channel with the increase in depth of flow, which shows that the percentage of flow in main channel decreases with the increase in depth of flow.

- The range of variation in velocity, in the floodplain region is found to decrease with the increase in the depth of flow while it is reverse in the main channel region.

Fig. 4.2.1 Depth flow in main channel (H) = 11.1 cm with U_p/U isovels

Fig. 4.2.2 Depth flow in main channel (H) = 11.7 cm with U_p/U isovels

Fig. 4.2.3 Depth flow in main channel (H) = 12 cm with U_p/U isovels
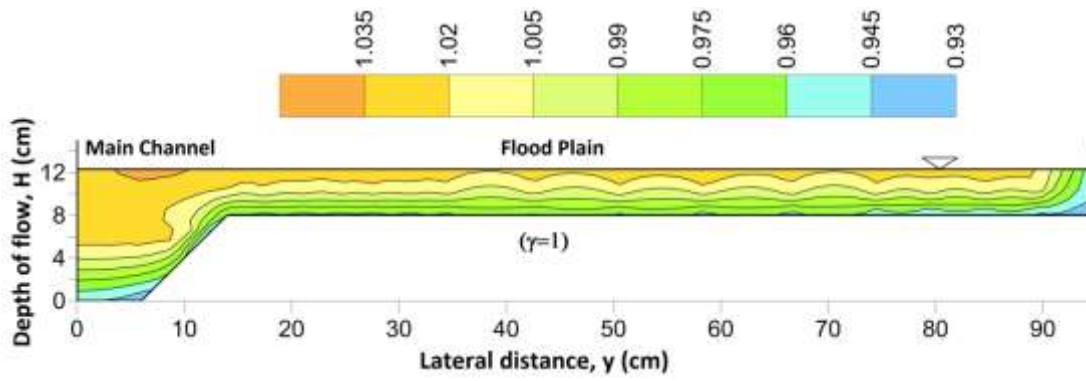
Fig. 4.2.4 Depth flow in main channel (*H*) = 12.3 cm with *U$_p$/U*

Fig. 4.2.5 Depth flow in main channel (*H*) = 12.6 cm with *U$_p$/U*
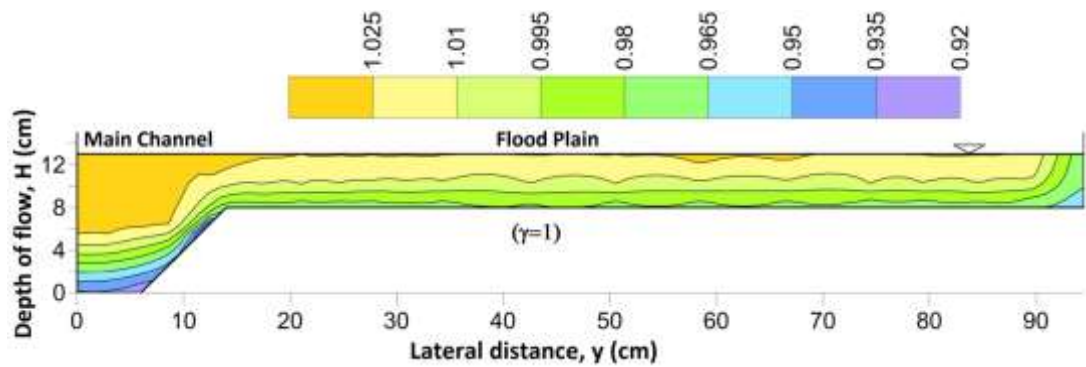
Fig. 4.2.6 Depth flow in main channel (*H*) = 13 cm with *U$_p$/U*
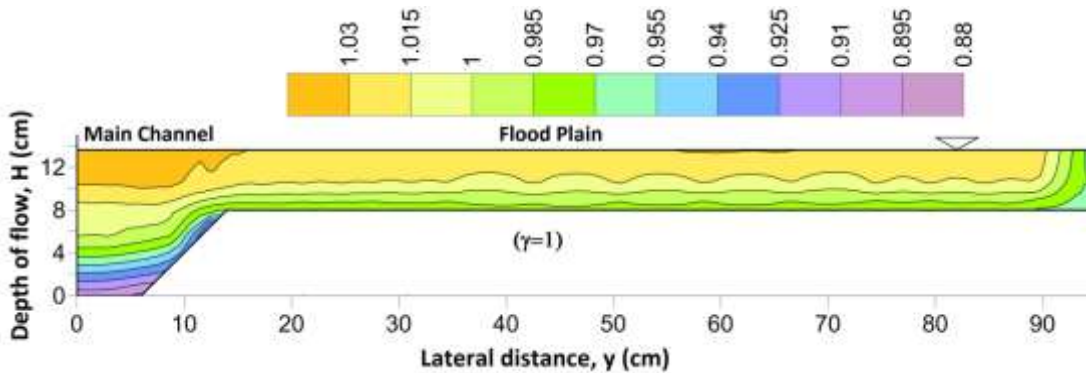
Fig. 4.2.7 Depth flow in main channel (*H*) =13.6 cm with *U$_p$/U*

Fig. 4.2 Dimensionless stream-wise velocity isovels of Smooth series ($\gamma = 1$)

From the observation of dimensionless stream-wise velocity contours of the Roughness-I (i.e. $\gamma = 1.12$), shown in Fig. 4.3.1-4.3.6, the following conclusions can be drawn.

- The velocity variation on floodplain gradually becomes stabilised with the increase in depth of flow.

- In each run, the maximum concentration of lower velocity contours is found on the floodplain.

- Here for $\gamma = 1.12$, the value of maximum velocity contours is found more than that of $\gamma = 1$ series.

- For $\gamma = 1.12$, the overall concentration of higher velocity contours in main channel is found more than that of $\gamma = 1$.

- The overall variation in velocity is found to decreases with increase in depth of flow.

Fig. 4.3.1 Depth flow in main channel (H) = 11.1 cm with U_p/U isovels

Fig. 4.3.2 Depth flow in main channel (H) = 11.6 cm with U_p/U isovels

Fig. 4.3.3 Depth flow in main channel (H) = 11.9 cm with U_p/U isovels

Fig. 4.3.4 Depth flow in main channel (H) = 12.4 cm with U_p/U isovels

Fig. 4.3.5 Depth flow in main channel (H) = 13 cm with U_p/U isovels

Fig. 4.3.6 Depth flow in main channel (H) = 13.5 cm with U_p/U isovels

Fig. 4.3 Dimensionless stream-wise velocity isovels of Roughness-I series ($\gamma = 1.12$)

From the observation of dimensionless stream-wise velocity contours of the Roughness-II (i.e. $\gamma = 1.32$), shown in Fig. 4.4.1-4.4.6, the following conclusions can be drawn.

- In each run, high concentration of lower velocity contours is found on the floodplain than on the main channel, but the limit of lowest velocity contour increases with increase in depth of flow. This concludes that the velocity fluctuation on the floodplain gradually becomes stabilised with the increase in depth of flow.

- The variation of velocity in main channel increases with increase in depth of flow.

- The concentration of maximum velocity contour is observed in the main channel and found to decreases with increase in depth of flow.

- The overall variation in velocity is found to decreases with increase in depth of flow.

- The limit of maximum velocity contour of this series is enough higher than the Smooth and Roughness-I series (i.e. $\gamma = 1$ and 1.12).
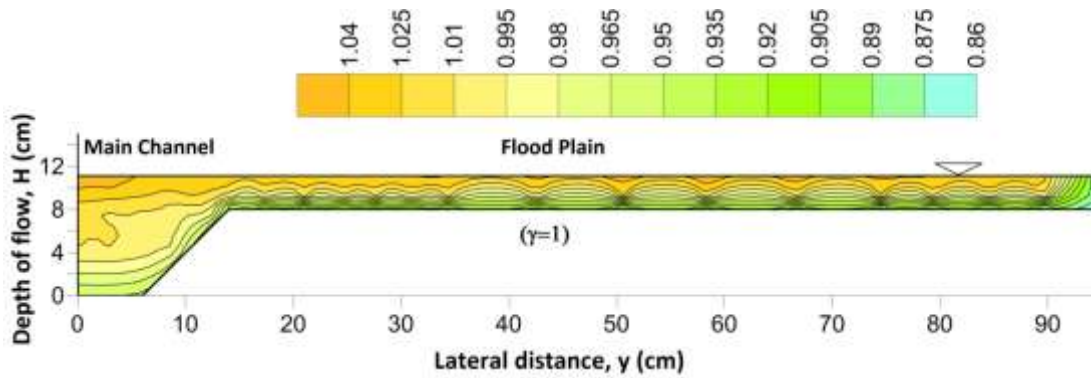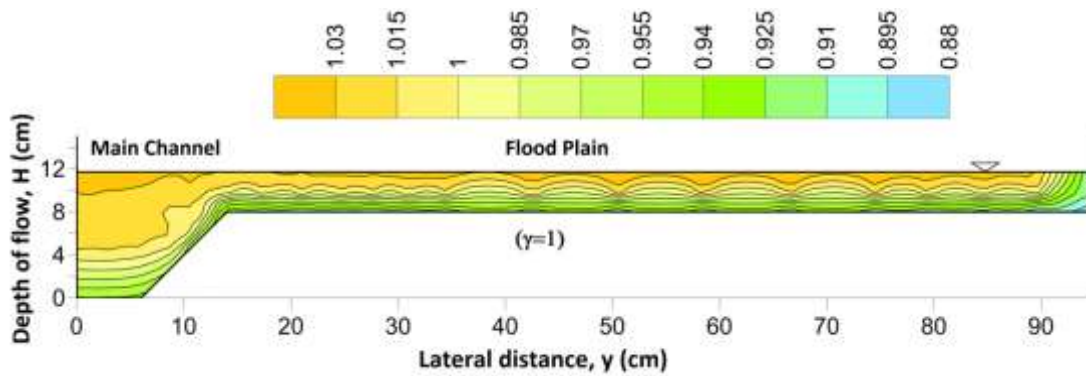

Fig. 4.4.1 Depth flow in main channel (H) = 11.6 cm with U_p/U isovels

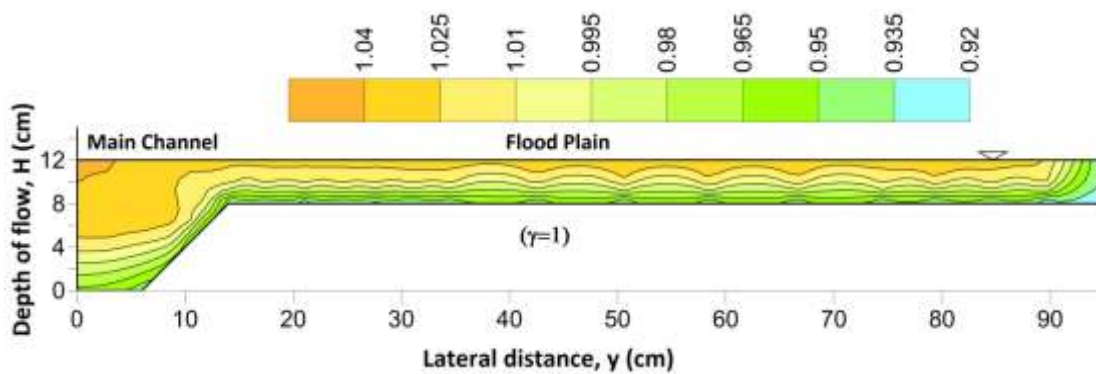**Fig. 4.4.2 Depth flow in main channel (H) = 12.1 cm with U_p/U isovels**
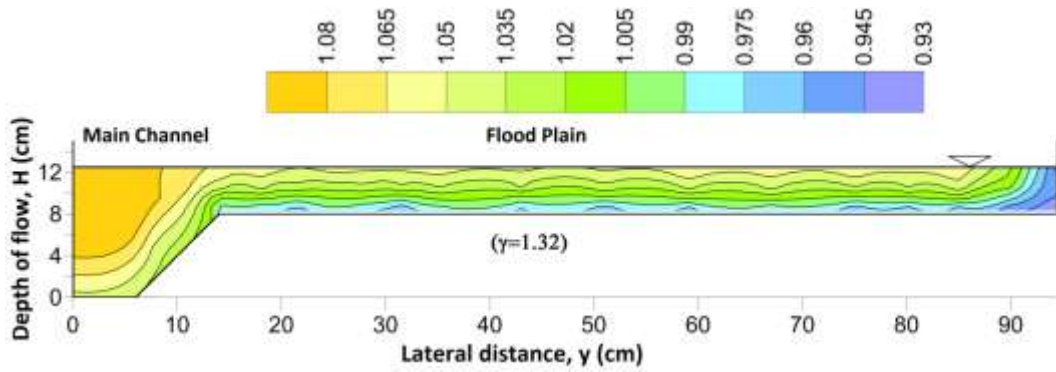
Fig. 4.4.3 Depth flow in main channel (*H*) = 12.5 cm with *U$_p$/U* isovels
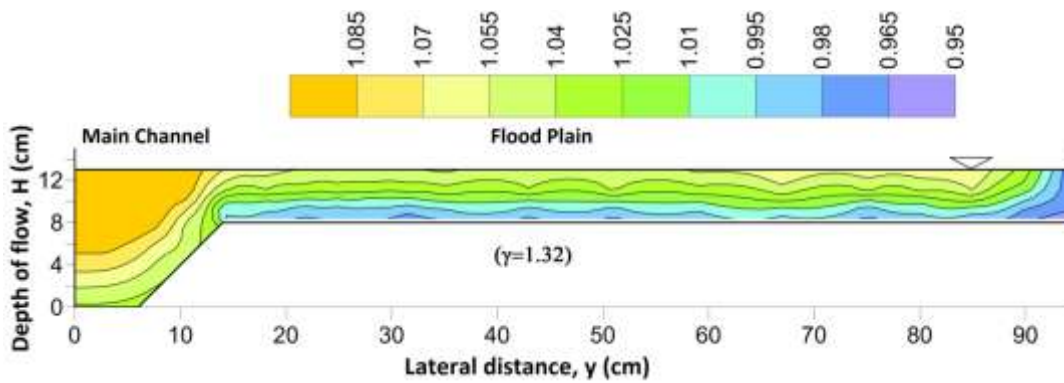
Fig. 4.4.4 Depth flow in main channel (*H*) = 13 cm with *U$_p$/U* isovels
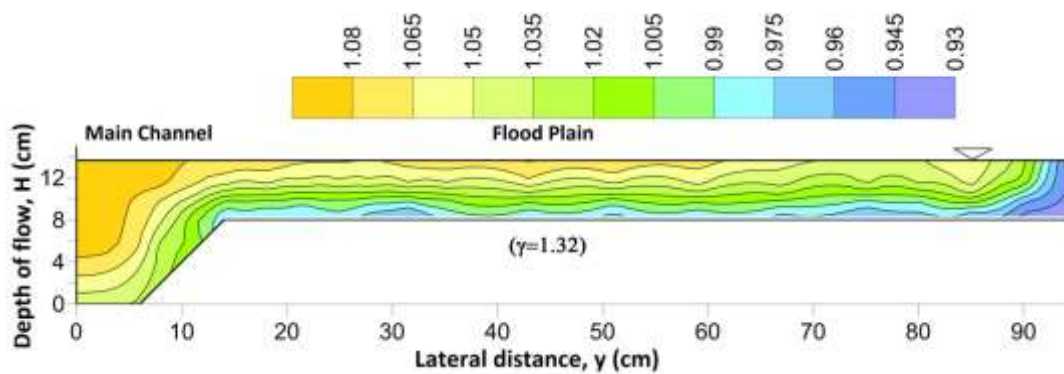
Fig. 4.4.5 Depth flow in main channel (*H*) = 13.65 cm with *U$_p$/U* isovels
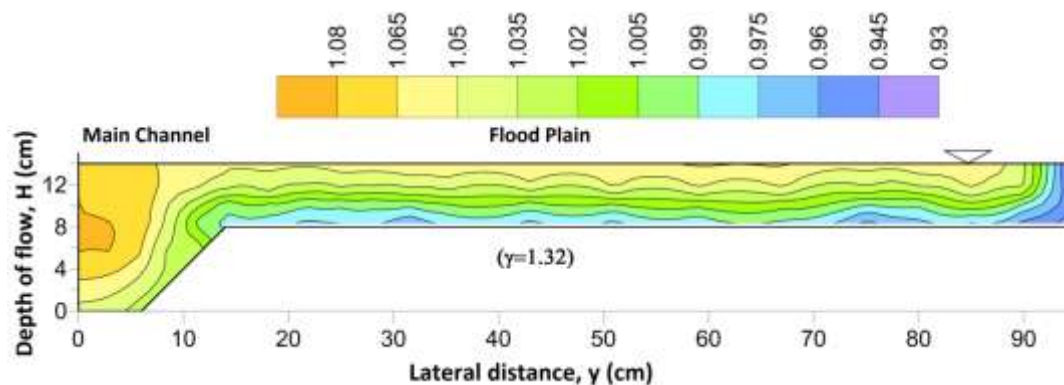
Fig. 4.4.6 Depth flow in main channel (*H*) = 14 cm with *U$_p$/U* isovels
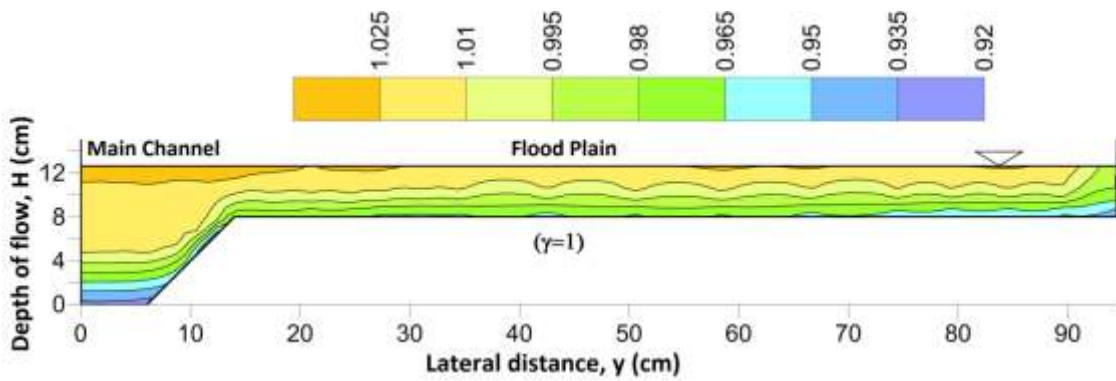
Fig. 4.4 Dimensionless stream-wise velocity isovels of Roughness-II series ($\gamma = 1.32$)

From the observation of dimensionless stream-wise velocity contours of the Roughness-III (i.e. $\gamma = 1.47$) shown in Fig. 4.5.1-4.5.6, the following conclusions can be drawn.

- The variation of velocity in main channel increases with increase in depth of flow.

- The concentration of higher velocity contours on floodplain gradually increases with the increase in depth of flow.

- In each run, the maximum concentration of lower velocity contours is found on the floodplain, which increases with increase in depth of flow.

- The limit of maximum velocity contours decreases with increase in depth of flow.

- The concentration of maximum velocity contours is found in the main channel and the concentration decreases with increase in depth of flow.

- Here the limit of maximum velocity contour is highest than the other three series.
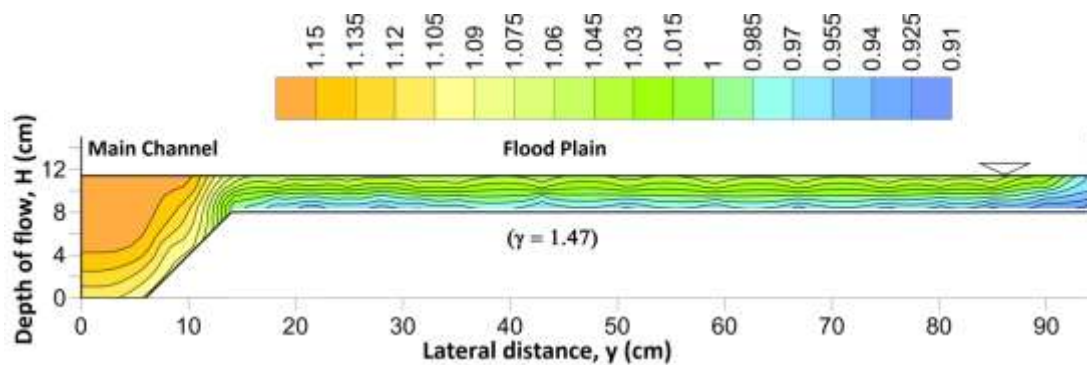
Fig. 4.5.1 Depth flow in main channel (*H*) = 11.4 cm with *U_p*/*U* isovels
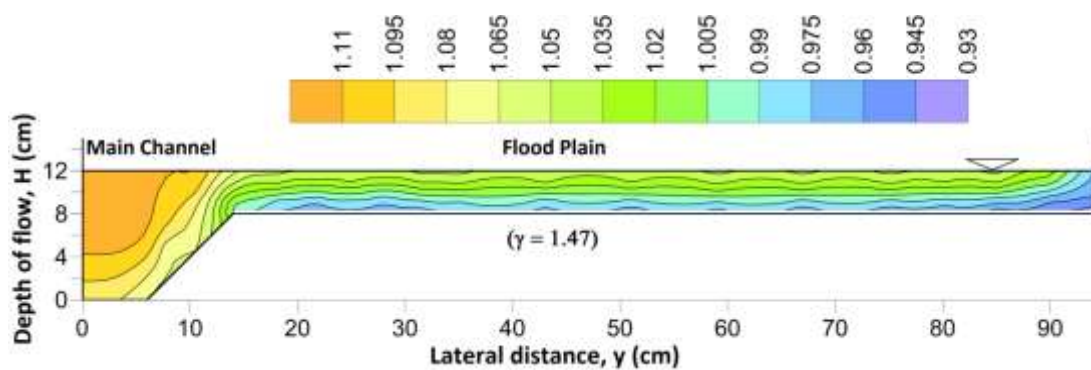
Fig. 4.5.2 Depth flow in main channel (*H*) = 12 cm with *U_p*/*U* isovels
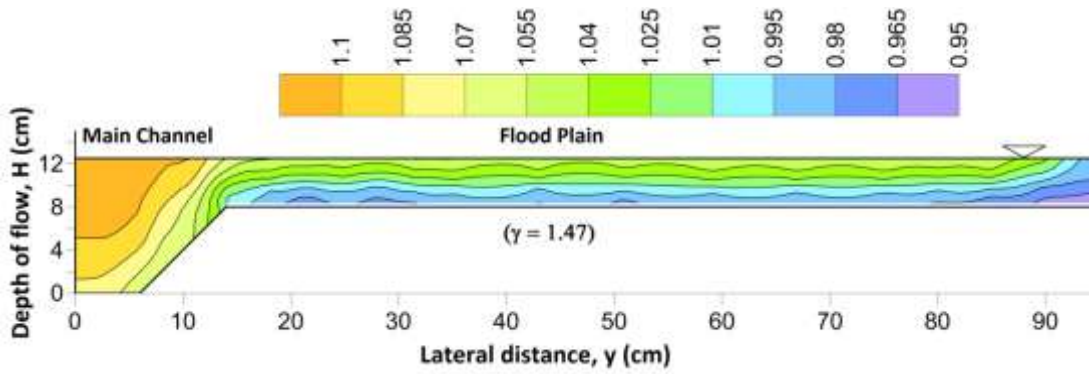
Fig. 4.5.3 Depth flow in Main Channel (*H*) = 12.5 cm with *U_p*/U isovels
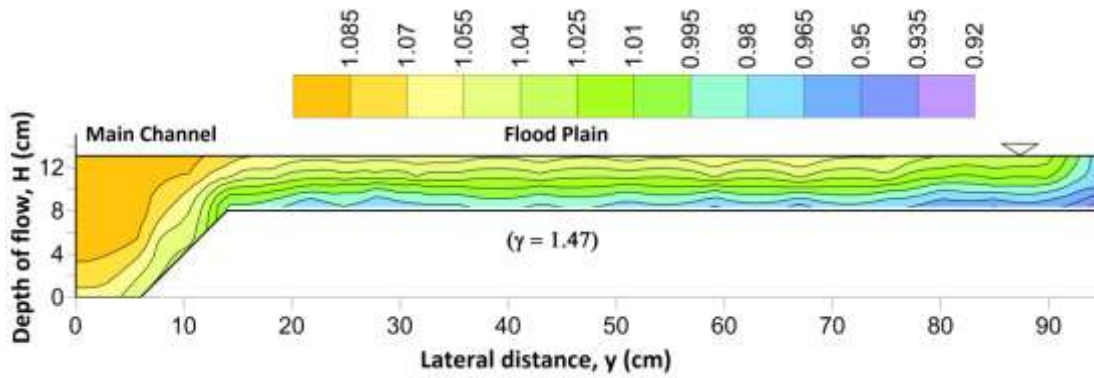
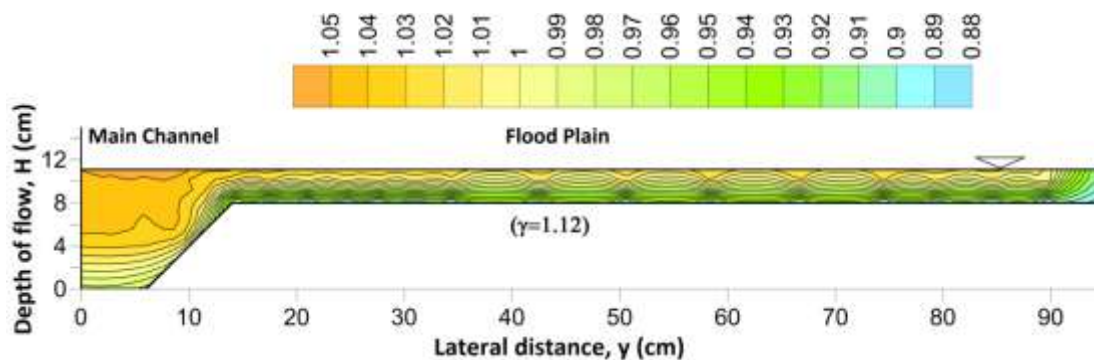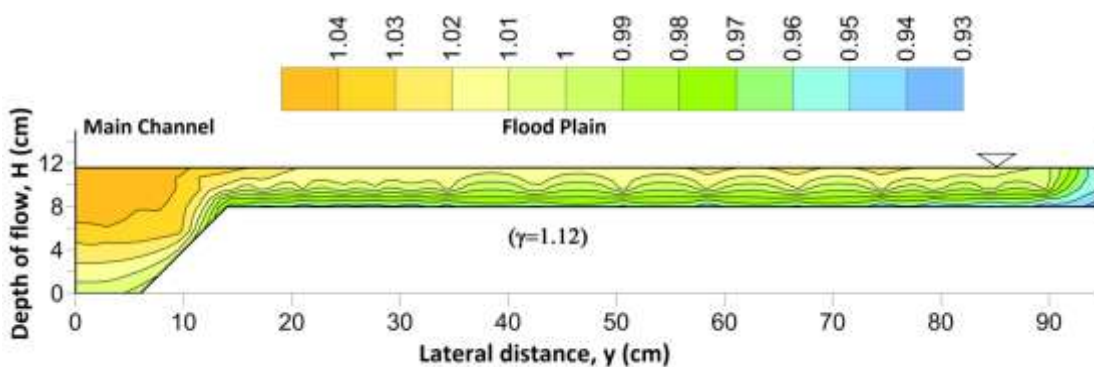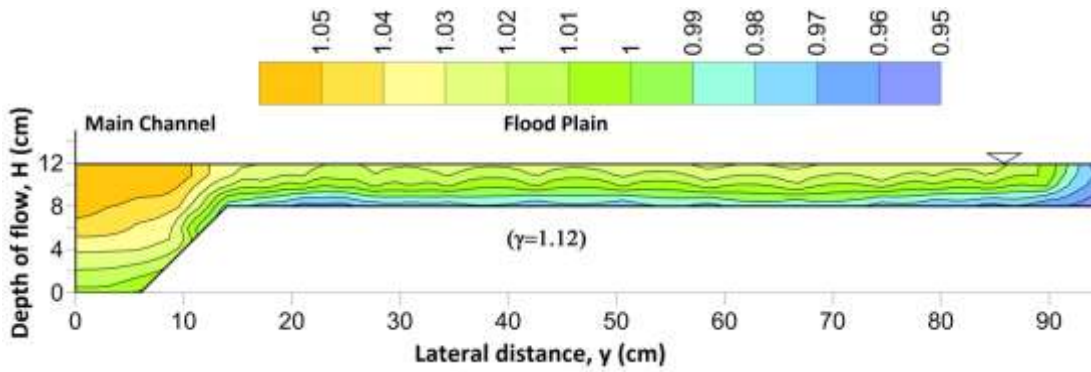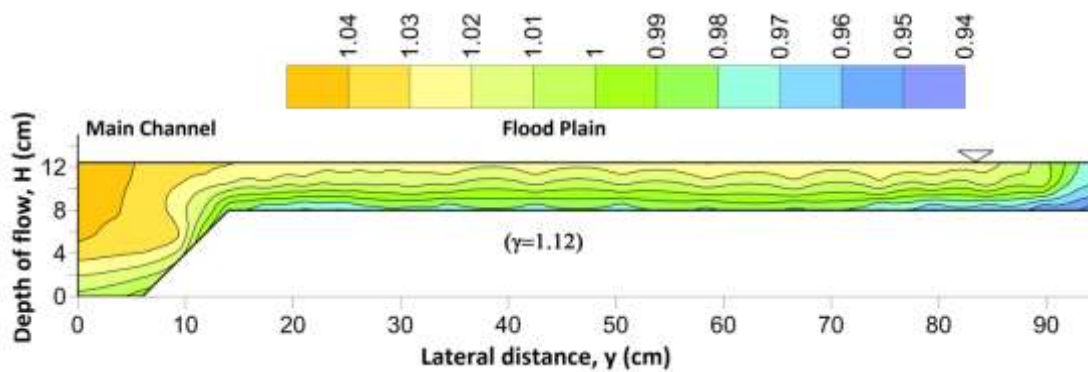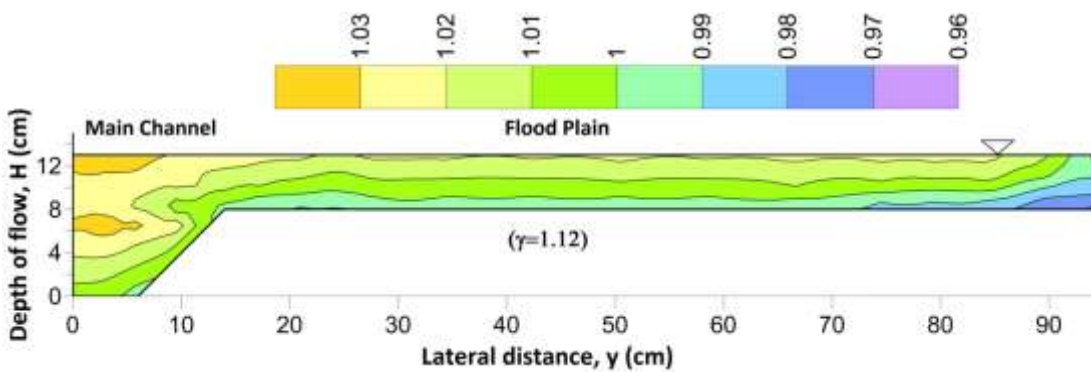**Fig. 4.5.4 Depth flow in Main Channel (*H*) = 13.05 cm with *U_p*/U isovels**

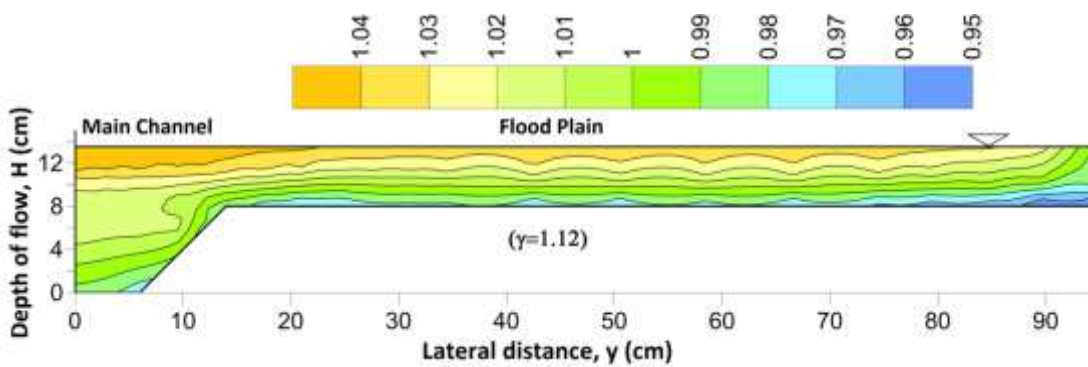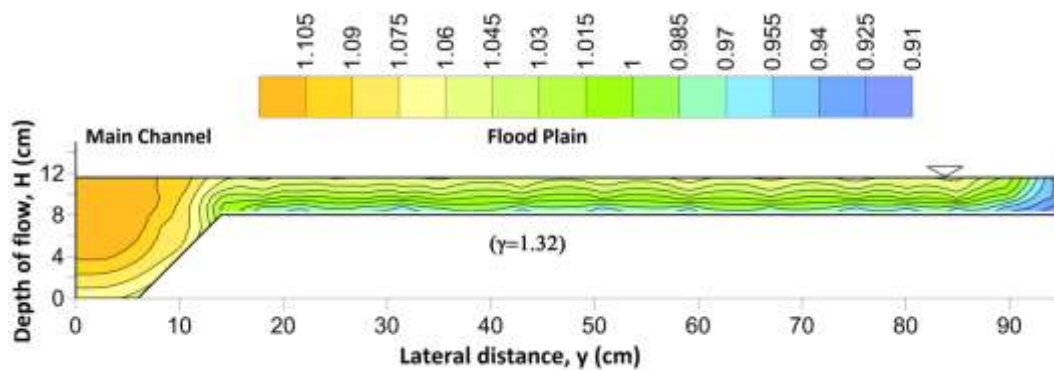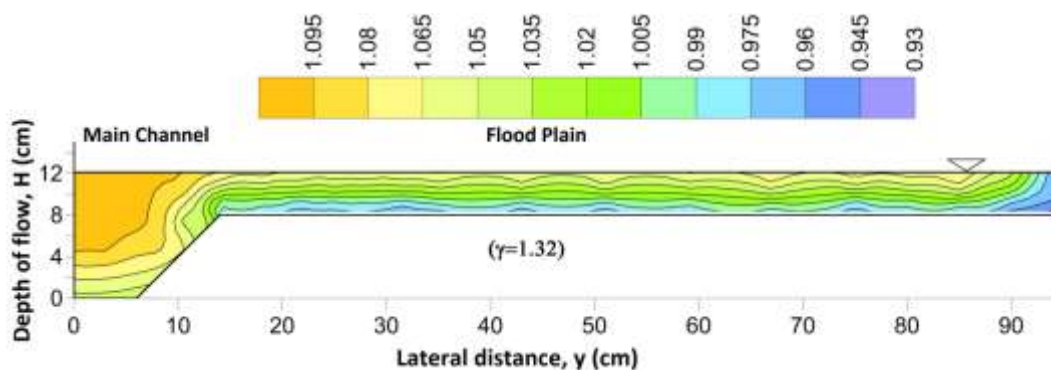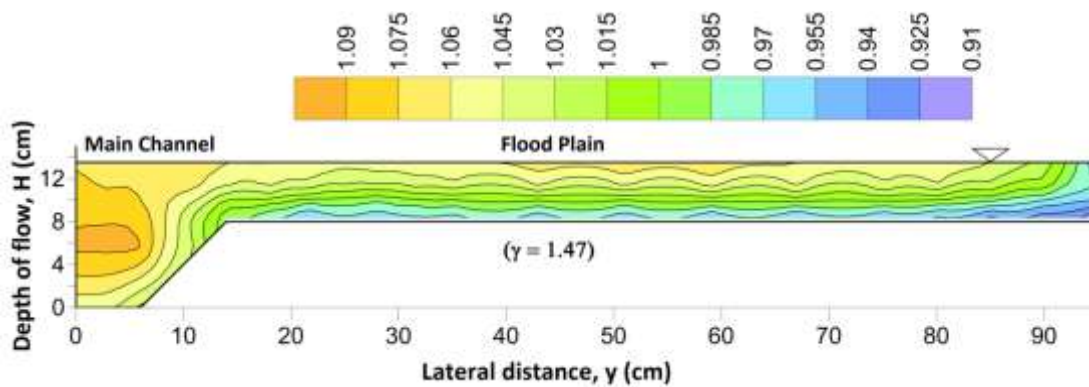**Fig. 4.5.5 Depth flow in Main Channel (*H*) = 13.5 cm with *U_p*/U isovels**
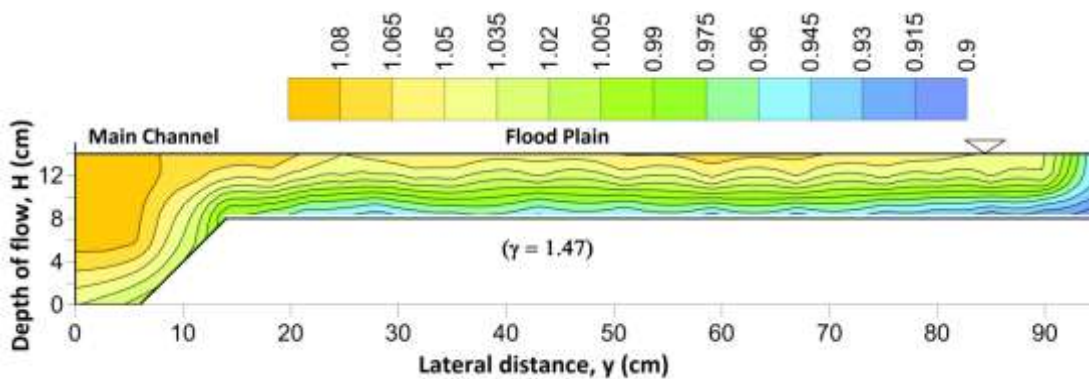
Fig. 4.5.6 Depth flow in Main Channel (*H*) = 14 cm with *U_p*/U isovels

Fig. 4.5 Dimensionless stream-wise velocity isovels of Roughness-III series (γ=1.47)

4.3   Evaluation of boundary shear stress

As boundary shear stress represents the local force by the fluid on a surface and is the main reason of sediment transport, erosion; it has a great importance in hydraulic research. There are several methods used to evaluate boundary shear stress in an open channel. The Preston tube technique has been popularly used in laboratory experiments as well as in field survey where the channel surface was either smooth or rough, Ackerman et al. (1994), Fernholz et al. (1996), Al-Khatib and Dmadi (1999), Atabey's Birmingham data [i]. In the present study this technique has been used to measure the boundary shear and for checking purpose energy gradient method has been used.

4.3.1   Energy gradient method

It is well established that for a regular prismatic channel under uniform flow conditions the sum of retarding boundary shear forces acting on the wetted perimeter must be equal to the resolved weight force along the direction of flow. Assuming the mean boundary shear stress (τ) to be constant over the entire boundary of the channel we can express (τ) as:

$$\tau = \rho g R S \tag{10}$$

where g = gravitational acceleration, ρ = density of flowing fluid, S = slope of the energy line, R = hydraulic radius of the channel cross section *(A/P), A* = area of channel cross section, and P = wetted perimeter of the channel section. This is known as energy gradient method. This method might not be suitable for local, small-scale estimates of the variations in shear stress due to the larger length requirement for the measurement of the energy slope (Babaeyan-Koopaei et al., 2002; Biron et al., 2004). Moreover, precise energy slope measurement is not always possible which eventually affects the accuracy of the method. For most of the cases, it is assumed that energy slope is equal to the bed slope which is necessarily not true in all flow conditions.

4.3.2   Preston tube technique

Based on the assumption of an inner law relating the local shear to the velocity distribution near the wall, Preston (1954), developed a simple technique for measuring local shear (τ_0) in a turbulent boundary layer using a pitot (preston) tube. The tube is placed in contact with the surface. Assessment of the near wall velocity distribution is empirically inferred from the differential pressure (Δp) between total and static pressure at the wall. The main difficulty of this method is obtaining the most appropriate

calibration equation or curve for the given tube diameter. Preston suggested a non-dimensional relationship between differential pressure (Δp) and local shear (τ_0) as:

$$\frac{\Delta p}{\rho}\frac{d^2}{\upsilon^2} = F\left[\frac{d^2\tau_0}{\rho\upsilon^2}\right] \tag{11}$$

where υ is kinematic viscosity of fluid, ρ is density of fluid and d is diameter of priston tube and functional relationship F needs to be determined. Preston proposed the following calibration equation

$$y' = 0.875x' - 1.396 \qquad\qquad \text{for} \qquad 4.1 \le x' \le 6.5 \tag{12}$$

where $x' = \log_{10}((\Delta P d^2)/(4\rho\upsilon^2))$ and $y' = \log_{10}((\tau_0 d^2)/(4\rho\upsilon^2))$.

Patel (1965), proposed a relationship for F in Eq. (11) valid in three ranges (y' between 1.5 -5.5).

$$y' = 0.5x' + 0.037 \qquad\qquad \text{for} \qquad y' \le 1.5 \tag{13.a}$$

$$y' = 0.8272 - 0.1381x' + 0.1437x'^2 - 0.006x'^3 \quad \text{for} \qquad 1.5 < y' \le 3.5 \tag{13.b}$$

$$x' = y' + 2\log_{10}(1.95y' + 4.10) \qquad\qquad \text{for} \qquad 3.5 < y' \le 5.5 \tag{13.c}$$

where υ, ρ, d denote the same as previous.

4.3.3 Boundary shear stress and Boundary shear force results

Boundary shear stress on different points of half of the wetted perimeter (as the compound channel was symmetrical) of the compound channel at test reach was obtained by Preston-tube technique. For example, calculation of boundary shear stress on different points (τ_i) of wetted perimeter for one of the Smooth series run (SMOB01) is shown in Table 7. In each series of overbank flow experiment, shear stress on each point of boundary was found out for different relative depth (β), (i.e. depth of flow on floodplain/ depth of flow on main channel bed). The observed experimental shear stress on each boundary point (τ_i) were multiplied by the appropriate wetted perimeter element to give boundary shear forces on each element of the wetted perimeter (SF_i), summation of which gives the total shear force acting on half of the wetted perimeter of the compound channel and by doubling up it we can get the total shear force acted on the whole wetted perimeter (SF_e). By this procedure SF_e was found out for all series of overbank flow (shown in Fig. 4.6). The observed mean shear stress (τ_e) further compared with the mean

shear stress (τ) value obtained by the energy gradient method, Eq. (10). The total shear force (*SF*) by using the mean shear stress obtained from energy gradient method has been calculated. The errors between τ_e and τ and the standard deviation of their mean has been tabulated in Table 6. The mean errors between τ_e and τ were found +5.75%, +3.87%, -6.94% and -5.37% with a standard deviation of 1.18, 1.07, 3.8 and 4.01, for series Smooth, Roughness-I, Roughness-II and Roughness-III respectively, which shows that the Preston-tube method approach agrees well with the mean value computed from the energy gradient approach. All the measured shear stress on each boundary point (τ_i) was multiplied with $\left(\tau / \tau_e \right)$ for error adjustment, so that when they were integrated they gave the correct energy gradient value.
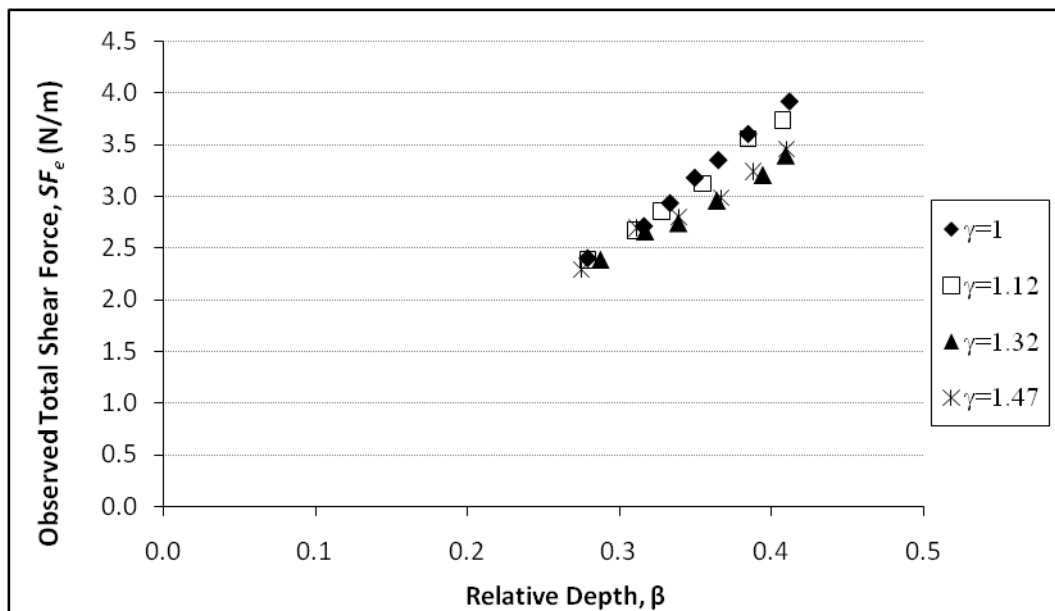
Fig. 4.6 Observed total shear force (*SF$_e$*) w.r.t. β of different series

Table 6. Comparison of the observed Boundary Shear Stress with the Boundary Shear obtained by the Energy Gradient Method

Series	Run No.	Relative depth (β)	Discharge, Q (m³/s)	Area of flow, A (m²)	Wetted Perimeter, P (m)	Hydraulic radius, R (m)	Mean shear stress by Energy Gradient method, τ (N/m²)	Mean shear force, SF (N/m)	Observed Mean shear stress, τ_e (N/m²)	Observed Mean shear force, SF_e (N/m)	Error as %	Mean Error	Standard deviation
Smooth	SMOB01	0.333	0.065	0.092	2.036	0.045	1.373	2.796	1.442	2.937	5.04	5.75	1.18
	SMOB03	0.316	0.060	0.086	2.030	0.042	1.292	2.623	1.337	2.715	3.52		
	SMOB04	0.350	0.071	0.097	2.042	0.048	1.454	2.969	1.558	3.182	7.17		
	SMOB05	0.385	0.083	0.111	2.056	0.054	1.640	3.372	1.752	3.603	6.83		
	SMOB06	0.365	0.075	0.103	2.048	0.050	1.534	3.142	1.636	3.352	6.68		
	SMOB07	0.279	0.049	0.075	2.018	0.037	1.128	2.276	1.192	2.405	5.66		
	SMOB08	0.412	0.096	0.122	2.068	0.059	1.798	3.718	1.894	3.917	5.33		
Roughness I	ROB100	0.407	0.091	0.120	2.066	0.058	1.772	3.661	1.808	3.735	2.04	3.87	1.07
	ROB101	0.328	0.060	0.090	2.034	0.044	1.346	2.738	1.401	2.850	4.10		
	ROB102	0.310	0.056	0.084	2.028	0.041	1.265	2.565	1.316	2.669	4.05		
	ROB104	0.355	0.068	0.099	2.044	0.049	1.480	3.026	1.526	3.120	3.08		
	ROB106	0.385	0.080	0.111	2.056	0.054	1.640	3.372	1.729	3.555	5.43		
	ROB107	0.279	0.047	0.075	2.018	0.037	1.128	2.276	1.179	2.379	4.50		
Roughness II	ROB201	0.317	0.055	0.089	2.038	0.044	1.336	2.723	1.308	2.667	-2.07	-6.94	3.8
	ROB202	0.288	0.047	0.080	2.028	0.039	1.200	2.435	1.179	2.391	-1.81		
	ROB203	0.339	0.062	0.097	2.046	0.047	1.443	2.954	1.342	2.745	-7.06		
	ROB204	0.395	0.081	0.119	2.069	0.057	1.748	3.617	1.552	3.212	-11.19		
	ROB206	0.410	0.088	0.125	2.076	0.060	1.839	3.819	1.639	3.403	-10.90		
	ROB207	0.364	0.070	0.106	2.056	0.052	1.577	3.242	1.441	2.964	-8.58		
Roughness III	ROB301	0.311	0.053	0.087	2.036	0.043	1.309	2.665	1.322	2.693	1.02	-5.37	4.01
	ROB302	0.410	0.091	0.125	2.076	0.060	1.839	3.819	1.663	3.452	-9.60		
	ROB303	0.388	0.080	0.116	2.066	0.056	1.709	3.531	1.567	3.238	-8.29		
	ROB305	0.339	0.062	0.097	2.046	0.047	1.443	2.954	1.367	2.798	-5.27		
	ROB306	0.367	0.071	0.107	2.057	0.052	1.590	3.271	1.449	2.982	-8.84		
	ROB307	0.275	0.045	0.076	2.024	0.038	1.146	2.319	1.132	2.291	-1.23		

Table 7. Calculation of Boundary Shear Stress (τ_i) of the Smooth series run (SMOB01)

		Cumulative Wetted Perimeter (m)	h_1 (m)	h_2 (m)	Δh	Δp	x'	y' <1.5	1.5< y' <3.5	3.5< y' <5.3	τ_i
B1	MC Bed	0.000	0.354	0.439	0.0850	239.108	6.5304	3.3022	4.3841	4.3280	1.5004
B2	MC Bed	0.030	0.3545	0.439	0.0845	237.047	6.5266	3.3003	4.3805	4.3247	1.4890
B3	MC Corner	0.060	0.357	0.4395	0.0825	228.802	6.5112	3.2926	4.3655	4.3111	1.4433
B4	MC Wall	0.128	0.355	0.439	0.0840	234.986	6.5228	3.2984	4.3768	4.3213	1.4776
B5	MC Wall	0.148	0.356	0.4395	0.0835	232.924	6.5190	3.2965	4.3731	4.3180	1.4662
B6	MC & FP Interface	0.173	0.356	0.4395	0.0835	224.679	6.5033	3.2887	4.3579	4.3042	1.4204
B7	FPlain	0.208	0.355	0.4395	0.0845	228.802	6.5112	3.2926	4.3655	4.3111	1.4433
B8	FPlain	0.243	0.3555	0.4395	0.0840	226.740	6.5073	3.2907	4.3617	4.3077	1.4319
B9	FPlain	0.278	0.3555	0.44	0.0845	228.802	6.5112	3.2926	4.3655	4.3111	1.4433
B10	FPlain	0.308	0.3555	0.4395	0.0840	226.740	6.5073	3.2907	4.3617	4.3077	1.4319
B11	FPlain	0.343	0.3555	0.4395	0.0840	226.740	6.5073	3.2907	4.3617	4.3077	1.4319
B12	FPlain	0.378	0.355	0.4395	0.0845	228.802	6.5112	3.2926	4.3655	4.3111	1.4433
B13	FPlain	0.458	0.3555	0.44	0.0845	228.802	6.5112	3.2926	4.3655	4.3111	1.4433
B14	FPlain	0.538	0.355	0.4395	0.0845	228.802	6.5112	3.2926	4.3655	4.3111	1.4433
B15	FPlain	0.618	0.3555	0.44	0.0845	228.802	6.5112	3.2926	4.3655	4.3111	1.4433
B16	FPlain	0.698	0.3555	0.44	0.0845	228.802	6.5112	3.2926	4.3655	4.3111	1.4433
B17	FPlain	0.778	0.3555	0.44	0.0845	228.802	6.5112	3.2926	4.3655	4.3111	1.4433
B18	FPlain	0.828	0.3555	0.4395	0.0840	226.740	6.5073	3.2907	4.3617	4.3077	1.4319
B19	FPlain	0.878	0.356	0.44	0.0840	226.740	6.5073	3.2907	4.3617	4.3077	1.4319
B20	FPlain	0.928	0.3565	0.4395	0.0830	222.618	6.4993	3.2867	4.3540	4.3007	1.4090
B21	FPCorner	0.978	0.357	0.4395	0.0825	220.557	6.4953	3.2847	4.3501	4.2971	1.3975
B22	FP Wall	0.994	0.3555	0.4365	0.0810	226.740	6.5073	3.2907	4.3617	4.3077	1.4319
B23	FP Wall	1.002	0.3555	0.437	0.0815	228.802	6.5112	3.2926	4.3655	4.3111	1.4433
B24	FP Wall	1.010	0.356	0.437	0.0810	226.740	6.5073	3.2907	4.3617	4.3077	1.4319
B25	FP Wall	1.018	0.356	0.437	0.0810	226.740	6.5073	3.2907	4.3617	4.3077	1.4319

Chapter 5

ANALYSIS And DISCUSSIONS Of The RESULTS

5 ANALYSIS AND DISCUSSION OF THE RESULTS

The primary aim of this research was to investigate the effect of the differential roughness on flow characteristics in compound channel having wide floodplains. Based on the analysis of the test results from the different series of experiments, a cumulative summary discussing the results and common findings of all the series of experiments are described in this chapter.

5.1 Distribution of Depth-Averaged Velocity

A general procedure for determining the depth-averaged velocity (U_d) is to average the velocity measured at $0.2d'$ and $0.8d'$ from the water surface, or the velocity measured at $0.6d'$ from the water surface (where d' = depth of flow on a surface), (Rantz et al., 1982). Following this, in the present study the depth-averaged velocity (U_d) was measured at $0.6d'$ from the water surface. The distribution of (U_d/U) across the dimensionless lateral distance (y/Y) for all relative depth (β) of all series of overbank flow experiments are shown in Fig. 5.1 series; where U is the mean velocity of respective run, y is the lateral distance of the point (at which the U_d was measured) from the middle of the main channel towards floodplain wall and Y is half of the compound channel width B (i.e. $Y = B/2$). From the figures it can be observed that:

- The variation in depth-averaged velocity, in main channel and flood plain region is minimum in case of $\gamma = 1$ with comparison to other three cases. The variation increases with the increase in differential roughness.

- In case of $\gamma = 1$, the overall depth-averaged velocity in the main channel region is lower than that of the flood plain for higher relative depth (β).

- The depth-averaged velocity in main channel decreases with the increase in relative depth (β) for all series of experiments, i.e. the resistance to the flow on floodplain by floodplain surface decreases with increase in differential roughness.

- The overall depth-averaged velocity in main channel increases with the increase in differential roughness (γ) (i.e. the percentage of flow increases with the increase in differential roughness), whereas decreases in floodplain region.

- Depth-averaged velocity near the wall increases with the increase in relative depth, i.e. the resistance to flow offered by the wall deceases with the increase in depth of flow as well as increase in differential roughness.
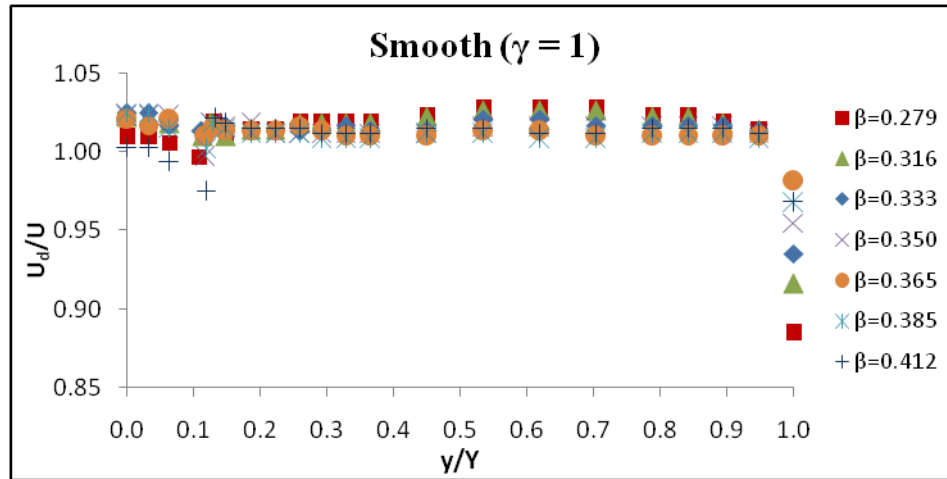
Fig. 5.1.1 Depth-Averaged velocity distribution of Smooth series
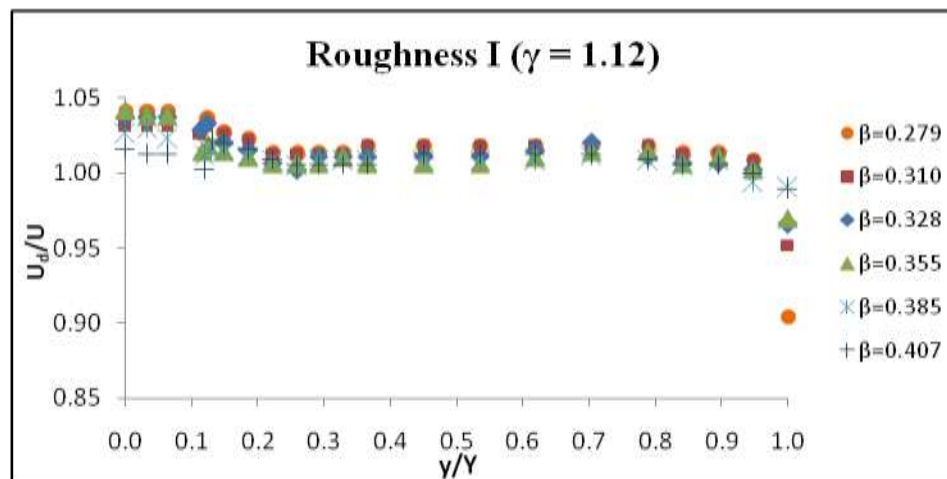
Fig. 5.1.2 Depth-Averaged velocity distribution of Roughness-I series
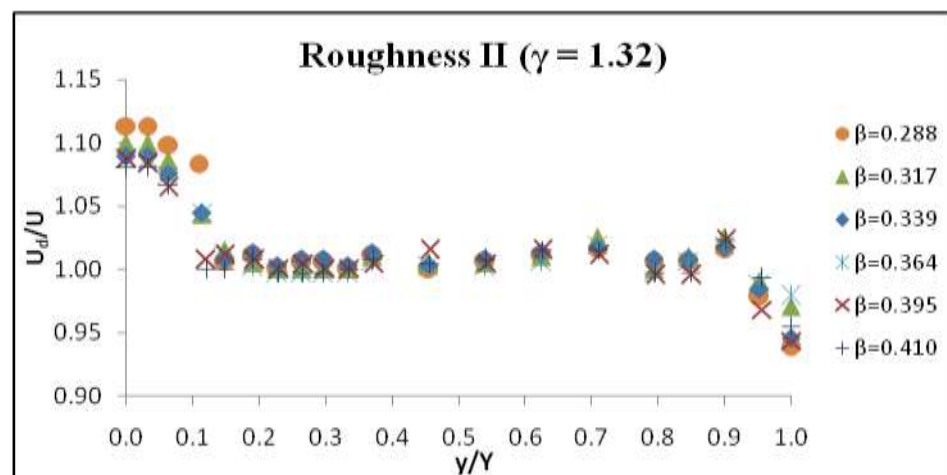
Fig. 5.1.3 Depth-Averaged velocity distribution of Roughness-II series
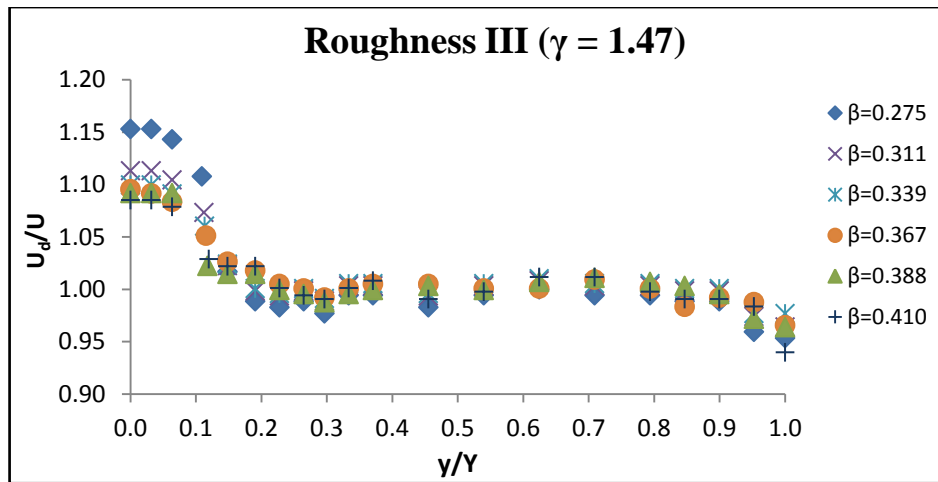
Fig. 5.1.4 Depth-Averaged velocity distribution of Roughness-III series

Fig. 5.1 Depth-Averaged velocity distribution of all series

5.2 Variation of Overall Manning's *n* and Zonal Manning's *n*

When the flow rises from the main channel to floodplain, the channel section becomes compound and a sudden change in hydraulic conditions such as area of flow, wetted perimeter, momentum transfer, surface roughness, etc. occurs, which gives rise to a sudden change in the resistance to the flow in the channel. Under such condition, Knight (1989), and Knight and Shino (1996) have shown that there is a large shear layers generated due to the difference in sub-area mean velocity in the main channel and that in the floodplain and it becomes the cause of abrupt change in overall Manning's *n* from inbank flow to overbank flow.

In the present study, to know the zonal *n* variation, the vertical divided channel method has been adopted in case of overbank flow. The zonal velocity of main channel (U_{mc}) and zonal velocity of floodplain (U_{fp}) are the average of depth-averaged velocity in main channel and floodplain respectively and are used in finding out experimental total discharge (Q_e). The mean error between actual discharge (Q_a) (given in section 4.1) and experimental total discharge (Q_e) is 2.76, 3.16, 4.77 and 4.40 with standard deviation of 1.44, 1.09, 0.82 and 1.51 for Smooth, Roughness-I, Roughness-II and Roughness-III series respectively. The U_{mc} and U_{fp} were adjusted by multiplying with (Q_a/Q_e) so that they will give actual discharge when will get multiplied with respective area. Now the Eq. (6) has been used to calculate the zonal as well as overall Manning's *n*. The overall Manning's *n*, of inbank and overbank flow is tabulated in Table 8. The zonal Manning's *n* of main channel (n_{zm}) and that of the floodplain (n_{zf}) for all series of overbank flow are

tabulated in Table 9. The variation of n, n_{zm} and n_{zf} w.r.t. dimensionless depth parameter (depth of flow on main channel, H / width of main channel base, b) for all the series of experiments are plotted in Fig. 5.2.1 – 5.2.4.

From Fig. 5.2 series, it can be observed that:

- The zonal roughness coefficient value of main channel (n_{zm}) is always more than that of flood plain (n_{zf}) in all series of experiments.

- Overall roughness coefficient (n) value, for overbank flow increases with increase in differential roughness value, i.e. with increase in roughness the resistance coefficient increases.

- In all series of experiments, a sudden decrease in overall n value for overbank flow just after the gradual increase in inbank flow, and then again gradual increase with increase in depth of flow is observed. The decrease of the overall n value in low depth overbank flow is mainly due to (i) sudden decrease in hydraulic radius and (ii) large amount of momentum transfer from main channel to floodplain. At higher overbank depths, the momentum transfer process is very less.

- A gradual increase in zonal roughness coefficient of floodplain (n_{zf}) value with increase in depth of flow is seen in all the series.

- The value of zonal roughness coefficient of the main channel (n_{zm}) in smooth series seems to be constant with increase in depth of flow. In case of Roughness-I and Roughness-II, initially the value slightly increases then decreases to become constant; whereas in case of Roughness-III, initially it increases then gradually decreases.
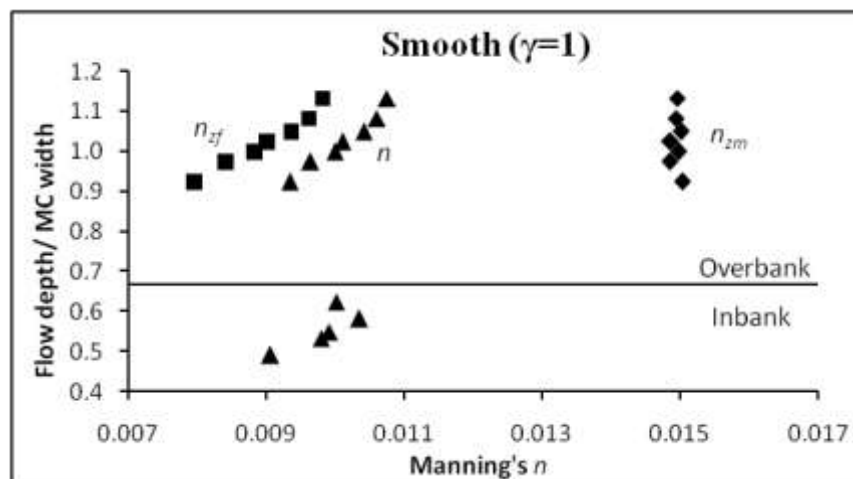
Fig. 5.2.1 Manning's *n* distribution of Smooth series
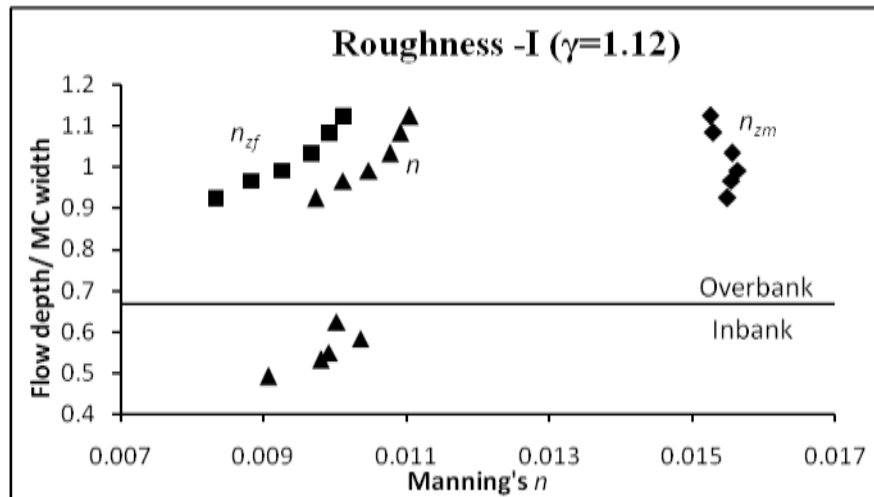
Fig. 5.2.2 Manning's n distribution of Roughness-I series
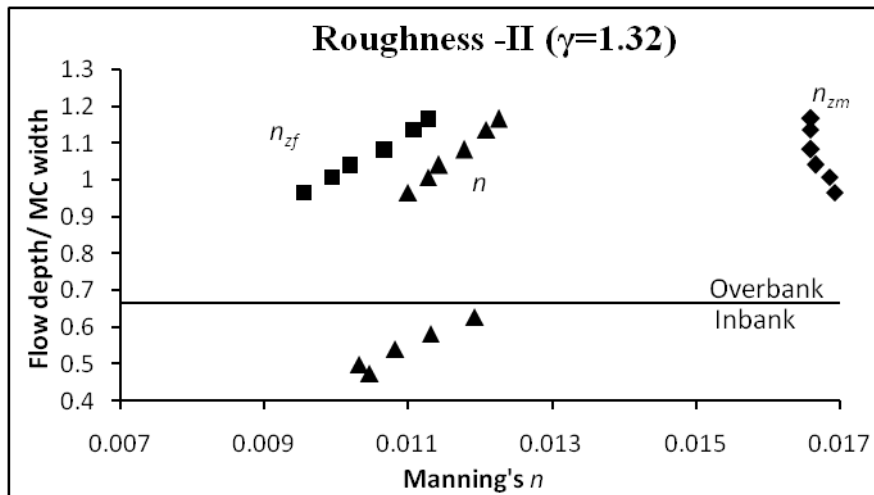
Fig. 5.2.3 Manning's *n* distribution of Roughness-II series
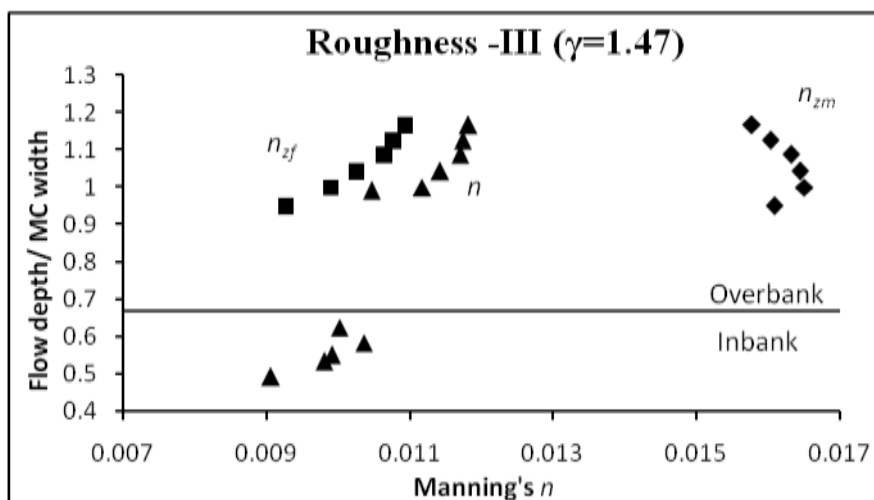
Fig. 5.2.4 Manning's *n* distribution of Roughness-III series

Fig. 5.2 Variation of Overall and Zonal Manning's *n*

Table 8. Variation of Overall Manning's _n_

Flow condition	Series	H/b	A (m²)	P (m)	R (m)	U (m/s)	_n_
*Inbank flow	Smooth, Roughness-I, Roughness-III	0.492	0.011	0.287	0.037	0.682	0.0091
		0.533	0.012	0.301	0.039	0.656	0.0098
		0.550	0.012	0.307	0.040	0.659	0.0099
		0.583	0.013	0.318	0.042	0.649	0.0104
		0.625	0.015	0.332	0.044	0.694	0.0100
	Roughness-II	0.475	0.010	0.281	0.036	0.580	0.0105
		0.500	0.011	0.290	0.037	0.603	0.0103
		0.542	0.012	0.304	0.040	0.599	0.0108
		0.583	0.013	0.318	0.042	0.594	0.0113
		0.629	0.015	0.334	0.044	0.585	0.0119
Overbank flow	Smooth	0.925	0.075	2.018	0.037	0.663	0.0093
		0.975	0.086	2.030	0.042	0.703	0.0096
		1.000	0.092	2.036	0.045	0.706	0.0100
		1.050	0.103	2.048	0.050	0.729	0.0104
		1.025	0.097	2.042	0.048	0.725	0.0101
		1.083	0.111	2.056	0.054	0.750	0.0106
		1.133	0.122	2.068	0.059	0.786	0.0108
	Roughness-I	0.925	0.075	2.018	0.037	0.636	0.0097
		0.967	0.084	2.028	0.041	0.660	0.0101
		0.992	0.090	2.034	0.044	0.665	0.0105
		1.033	0.099	2.044	0.049	0.689	0.0108
		1.083	0.111	2.056	0.054	0.728	0.0109
		1.125	0.120	2.066	0.058	0.757	0.0110
	Roughness-II	0.967	0.080	2.028	0.039	0.587	0.0110
		1.008	0.089	2.038	0.044	0.614	0.0113
		1.042	0.097	2.046	0.047	0.639	0.0114
		1.083	0.106	2.056	0.052	0.657	0.0118
		1.138	0.119	2.069	0.057	0.686	0.0121
		1.167	0.125	2.076	0.060	0.700	0.0123
	Roughness-III	0.950	0.076	2.024	0.038	0.590	0.0106
		1.000	0.087	2.036	0.043	0.612	0.0112
		1.042	0.097	2.046	0.047	0.639	0.0114
		1.088	0.107	2.057	0.052	0.665	0.0117
		1.125	0.116	2.066	0.056	0.696	0.0117
		1.167	0.125	2.076	0.060	0.726	0.0118

*For Smooth, Roughness-I and Roughness-III series, the main channel was smooth; therefore a single inbank flow experiment was carried out for all. In Roughness-II series, the main channel was mesh roughened; for which another inbank flow experiment was carried out.

Table 9. Variation of Zonal Manning's *n*

Series	H/b	A_{mc} (m²)	P_{mc} (m)	R_{mc} (m)	U_{mc} (m/s)	n_{zm}	A_{fp} (m²)	P_{fp} (m)	R_{fp} (m)	U_{fp} (m/s)	n_{zf}
Smooth	0.925	0.025	0.346	0.071	0.638	0.0150	0.050	1.672	0.030	0.675	0.0080
	0.975	0.026	0.346	0.076	0.675	0.0148	0.060	1.684	0.035	0.715	0.0084
	1.000	0.027	0.346	0.079	0.683	0.0150	0.064	1.690	0.038	0.716	0.0088
	1.025	0.028	0.346	0.081	0.703	0.0148	0.069	1.696	0.041	0.734	0.0090
	1.050	0.029	0.346	0.083	0.710	0.0150	0.074	1.702	0.044	0.737	0.0094
	1.083	0.030	0.346	0.087	0.731	0.0149	0.081	1.710	0.047	0.756	0.0096
	1.133	0.032	0.346	0.091	0.758	0.0150	0.090	1.722	0.052	0.795	0.0098
Roughness I	0.925	0.025	0.346	0.071	0.619	0.0155	0.050	1.672	0.030	0.645	0.0083
	0.967	0.026	0.346	0.075	0.640	0.0155	0.058	1.682	0.034	0.670	0.0088
	0.992	0.027	0.346	0.078	0.650	0.0156	0.063	1.688	0.037	0.672	0.0093
	1.033	0.028	0.346	0.082	0.676	0.0156	0.071	1.698	0.042	0.695	0.0097
	1.083	0.030	0.346	0.087	0.714	0.0153	0.080	1.710	0.047	0.734	0.0099
	1.125	0.031	0.346	0.091	0.738	0.0152	0.089	1.720	0.051	0.764	0.0101
Roughness II	0.967	0.026	0.352	0.074	0.582	0.0169	0.054	1.677	0.032	0.589	0.0096
	1.008	0.027	0.352	0.078	0.605	0.0169	0.062	1.687	0.037	0.619	0.0099
	1.042	0.029	0.352	0.081	0.629	0.0167	0.068	1.695	0.040	0.643	0.0102
	1.083	0.030	0.352	0.085	0.652	0.0166	0.076	1.705	0.045	0.659	0.0107
	1.138	0.032	0.352	0.091	0.678	0.0166	0.087	1.718	0.050	0.688	0.0111
	1.167	0.033	0.352	0.093	0.692	0.0166	0.092	1.725	0.054	0.703	0.0113
Roughness III	0.950	0.026	0.352	0.073	0.604	0.0161	0.050	1.673	0.030	0.584	0.0093
	1.000	0.027	0.352	0.077	0.614	0.0165	0.060	1.685	0.036	0.611	0.0099
	1.042	0.029	0.352	0.081	0.637	0.0164	0.068	1.695	0.040	0.639	0.0102
	1.088	0.030	0.352	0.086	0.665	0.0163	0.077	1.706	0.045	0.666	0.0106
	1.125	0.031	0.352	0.089	0.696	0.0160	0.084	1.715	0.049	0.696	0.0108
	1.167	0.033	0.352	0.093	0.728	0.0158	0.092	1.725	0.054	0.725	0.0109

5.3 Variation in Distribution of Flow

Discharge carried by the main channel is generally calculated by separating from the compound section by vertical divided channel method. The flow in main channel was obtained by numerically integrating the depth-averaged velocity of main channel and then multiplying the integrated value with the area of main channel. Due to transfer of momentum between floodplain and main channel, the percentage of flow carried by the main channel with depth does not follow simple area ratios. At lower depths of flow over floodplain, the percentage of flow in main channel (*%Q_{mc}*) is more than that of at higher depths of flow on the same. In past, the flow and velocity distribution in compound sections have been investigated by many investigators (Knight and Demetriou (1983), Wormleaton and Hadjipanos (1985), Myer (1987), Atabay and Knight (2002), Yang et al. (2004), Hin and Bessaih (2004), Khatua (2008), Absi (2011), Khatua et al. (2012)). In the

present study, the variation of ($\%Q_{mc}$) with the variation in differential roughness was found out and is shown in Fig. 5.3. In the figure, we can see that with the increase in relative depth, the percentage of flow in main channel ($\%Q_{mc}$) decreases due to the effect of momentum transfer between floodplain and main channel decreasing with the increase in the depth of flow. In the figure, we can also observe that the percentage of flow in main channel ($\%Q_{mc}$) increases with the increase in differential roughness (γ) which may be due to the resistance to flow offered by floodplain in comparison to main channel increasing with the increase in differential roughness value (as main channel is smoother than the floodplain).
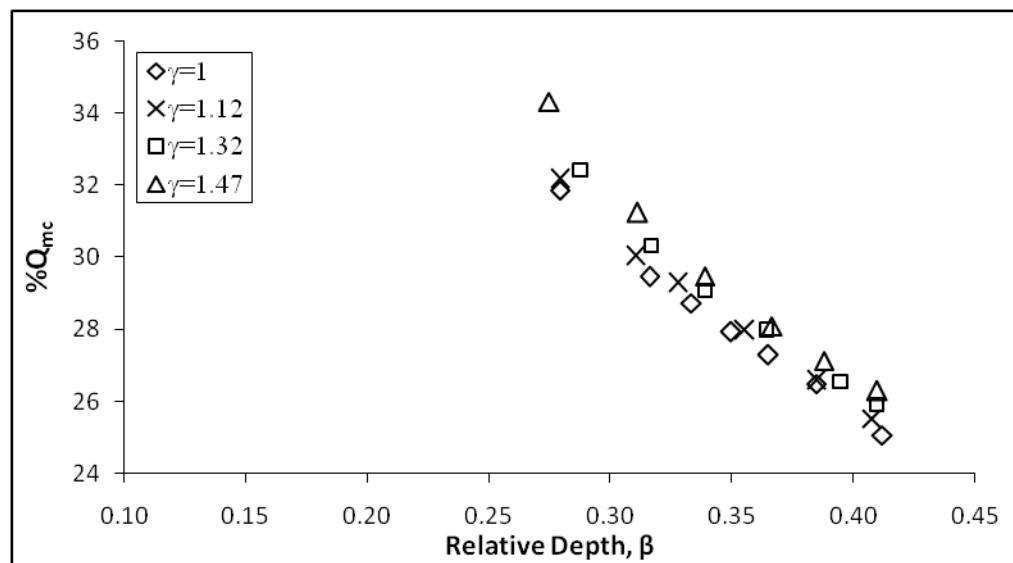
Fig. 5.3 Variation in distribution of flow due to differential roughness

5.4 Distribution of Boundary Shear Force

Many investigators found that the boundary shear stress distribution is not uniform over the wetted perimeter (Knight and Demetriou (1983), Knight and Hamed (1984), Al-Khatib & Dmadi (1999), Khatua and Patra (2007), Kean et al. (2009), Knight et al. (2010), Khatua et al. (2012)). Still boundary shear distribution in compound channel having width ratio (α) > 10 along with roughness variation is rare to come across. This research deals with the effect of wide floodplains and the differential roughness on the evaluation of boundary shear distribution stress carried by the channel boundary.

To estimate the boundary shear distribution, the boundary shear force on each element of the wetted perimeter (SF_i) of floodplain was obtained by multiplying the adjusted shear stress on each point (τ_i) (section 4.3.3) with appropriate wetted perimeter

element of floodplain, then all were integrated and then doubled to give total shear force carried by the floodplains (SF_{fp}). Then the $\%SF_{fp}$ was calculated from total shear force (SF). The percentage of shear force carried by floodplains ($\%SF_{fp}$) was calculated for different relative depth of all series experiment, (Table 10).

Table 10. Observed Percentage of Shear Force carried by Floodplains in all the Series of Overbank Flow

Series	Run No.	Differential roughness, γ	Relative depth, β	Discharge, Q (m³/s)	Experimental percentage of shear force carries by floodplains, $\%SF_{fp}$
Smooth	SMOB07	1	0.279	0.0494	81.23
	SMOB03	1	0.316	0.0604	82.14
	SMOB01	1	0.333	0.0647	82.65
	SMOB04	1	0.350	0.0706	83.45
	SMOB06	1	0.365	0.0751	83.88
	SMOB05	1	0.385	0.0828	84.38
	SMOB08	1	0.412	0.0957	84.99
Roughness I	ROB107	1.12	0.279	0.0475	80.95
	ROB102	1.12	0.310	0.0555	81.76
	ROB101	1.12	0.328	0.0597	82.19
	ROB104	1.12	0.355	0.0683	82.39
	ROB106	1.12	0.385	0.0805	82.91
	ROB100	1.12	0.407	0.0908	83.00
Roughness II	ROB202	1.32	0.288	0.0468	80.13
	ROB201	1.32	0.317	0.0548	80.88
	ROB203	1.32	0.339	0.0618	81.25
	ROB207	1.32	0.364	0.0698	81.48
	ROB204	1.32	0.395	0.0813	81.64
	ROB206	1.32	0.410	0.0876	81.64
Roughness III	ROB307	1.47	0.275	0.0449	79.18
	ROB301	1.47	0.311	0.0535	80.27
	ROB305	1.47	0.339	0.0618	80.79
	ROB306	1.47	0.367	0.0713	81.03
	ROB303	1.47	0.388	0.0805	81.15
	ROB302	1.47	0.410	0.0908	81.18

The variation in percentage of shear force carried by floodplains ($\%SF_{fp}$) of compound channels having different differential roughness (γ) is shown in Fig. 5.4. In the following figure it can be observed that:

- The percentage of shear force carried by floodplains ($\%SF_{fp}$) gradually increases with the increase in relative depth (β) in all the cases (i.e. for $\gamma = 1$, 1.12, 1.32 and 1.47).

- The increment of $\%SF_{fp}$ w.r.t. β gradually decreases with the increase in differential roughness (γ). This may be due to the surface roughness, which reduces the velocity of flow on floodplain resulting in the decrease in shear force (as shear force is dependent of velocity). Simultaneously it increases the velocity in the main channel.
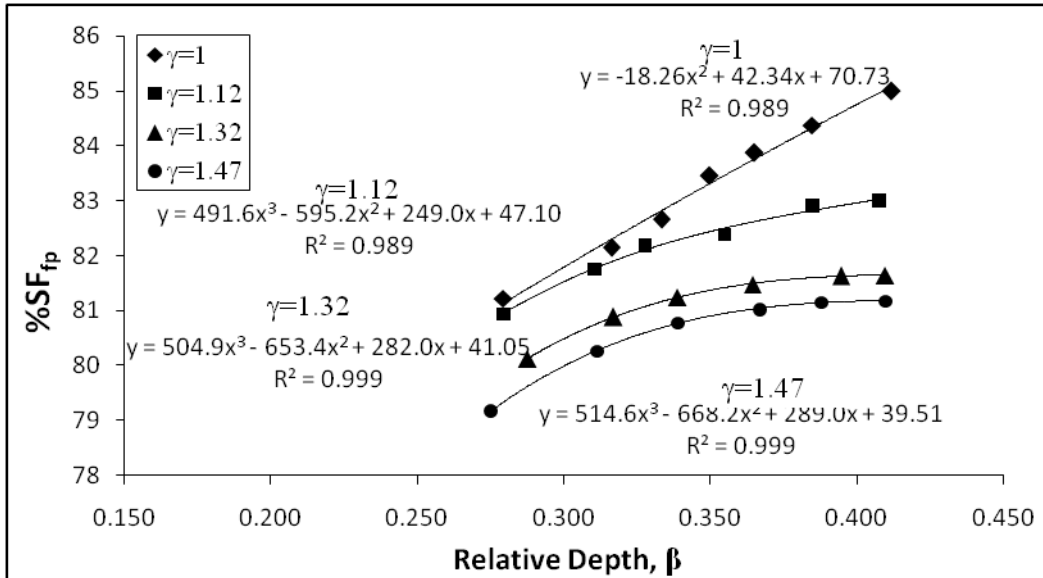
Fig. 5.4 Variation of $\%SF_{fp}$ w.r.t. β for different γ values

5.5 Development of Boundary Shear Distribution Model

Knight and Hamed (1984) investigated boundary shear force distribution for a compound channel, whose floodplain was roughened by strip roughness. To study the effect of differential roughness between the floodplains and the main channel, the distance between strip roughness materials was varied for the floodplains while the main channel was kept smooth. They proposed equation for the percentage of total shear force carried by the floodplain ($\%SF_{fp}$) as:

$$\%SF_{fp} = 48(\alpha - 0.8)^{0.289}(2\beta)^{1/m}(1 + 1.02\sqrt{\beta}\log\gamma) \qquad (14.a)$$

where m can be calculated from the relation $m = 1/(0.75e^{0.38\alpha})$ \qquad (14.b)

in which α = width ratio of the compound channel (B/b), B = width of compound channel, b = width of main channel base, β = relative depth (h/H), H = depth of flow on the main channel, h = depth of flow on the floodplain, γ = differential roughness (the ratio of Manning's resistance coefficient of the floodplain boundary (n_{fp}) to that of the main channel boundary (n_{mc})). This equation was developed for low width ratio ($\alpha = 4$) and for $1 \leq \gamma \leq 3$.

Further due to complexity of the empirical Eq. (14), Khatua & Patra, (2007) modified Eq. (14) to a simple equation for predicting the percentage of floodplain shear force carries by floodplains in compound channel having different roughness in main channel and floodplain surface for a range $2 \leq \alpha \leq 4$, as:

$$\%SF_{fp} = 1.23\beta^{0.1833}(38Ln\alpha + 3.6262)[1 + 1.02\sqrt{\beta}\log\gamma] \qquad (15)$$

where α, β and γ are same as defined for the Eq. (14). Using Eq. (14) and (15), the $\%SF_{fp}$ has been calculated for the present data series ($\alpha = 15.75$) (shown in Table 11) and compared with the observed value obtained from the experiments. It can be noticed that these equations estimate $\%SF_{fp}$ more than 100% which is quite unforeseen.

The Khatua et al. (2012), proposed equation to predict $\%SF_{fp}$ for compound channel, when they found Eq. (14) and (15) give errors more than 70% for $\alpha = 6.67$. They proposed an equation for $\%SF_{fp}$ as a function of $\%A_{fp}$, which was further converted in terms of α and β as

$$\%SF_{fp} = 4.105\left[\frac{100\beta(\alpha-1)}{1+\beta(\alpha-1)}\right]^{0.6917} \qquad (16)$$

where α and β are same as defined for the Eq. (14). The Eq. (16) was meant for compound channel having homogeneous roughness (i.e. $\gamma = 1$).

Table 11. Estimation of Percentage of Shear Force carried by the Floodplains in all the series of Overbank Flow

Series	Run No.	Differential roughness, γ	Relative depth, β	Discharge, Q (m³/s)	Percentage of shear force carries by floodplains, $\%SF_{fp}$		
					Observed	By Equation (14)	By Equation (15)
Smooth	SMOB07	1	0.279	0.0494	81.23	104.68	105.52
	SMOB03	1	0.316	0.0604	82.14	104.72	107.95
	SMOB01	1	0.333	0.0647	82.65	104.74	109.00
	SMOB04	1	0.350	0.0706	83.45	104.76	109.95
	SMOB06	1	0.365	0.0751	83.88	104.77	110.83
	SMOB05	1	0.385	0.0828	84.38	104.79	111.90
	SMOB08	1	0.412	0.0957	84.99	104.82	113.30
Roughness I	ROB107	1.12	0.279	0.0475	80.95	107.38	108.24
	ROB102	1.12	0.310	0.0555	81.76	107.56	110.50
	ROB101	1.12	0.328	0.0597	82.19	107.66	111.69
	ROB104	1.12	0.355	0.0683	82.39	107.80	113.46
	ROB106	1.12	0.385	0.0805	82.91	107.96	115.28
	ROB100	1.12	0.407	0.0908	83.00	108.07	116.60
Roughness II	ROB202	1.32	0.288	0.0468	80.13	111.61	113.10
	ROB201	1.32	0.317	0.0548	80.88	111.99	115.49
	ROB203	1.32	0.339	0.0618	81.25	112.27	117.17
	ROB207	1.32	0.364	0.0698	81.48	112.57	119.03
	ROB204	1.32	0.395	0.0813	81.64	112.92	121.13
	ROB206	1.32	0.410	0.0876	81.64	113.09	122.13
Roughness III	ROB307	1.47	0.275	0.0449	79.18	114.12	114.72
	ROB301	1.47	0.311	0.0535	80.27	114.77	117.97
	ROB305	1.47	0.339	0.0618	80.79	115.24	120.27
	ROB306	1.47	0.367	0.0713	81.03	115.69	122.48
	ROB303	1.47	0.388	0.0805	81.15	116.02	124.07
	ROB302	1.47	0.410	0.0908	81.18	116.36	125.66

In the present study, the same dimensionless parameters (α, β and γ, in Eq. (14) and (15)) are taken into consideration for boundary shear distribution modelling (i.e. $\%SF_{fp}$ calculation). For better understanding of the variation of percentage of floodplain shear force with respect to differential roughness, α was kept constant ($\alpha = 15.75$) for all the series of experiments (i.e. for $\gamma = 1$, 1.12, 1.32 & 1.47) conducted in this research. The variation of $\%SF_{fp}$ w.r.t. β for different γ values with smooth curve equations is shown in Fig. 5.3. Now using Eq. (16), which was meant for homogeneous roughness, $\%SF_{fp}$ has been calculated for all series of experiments and then compared with the observed value (tabulated in Table 12).

Table 12. Comparison of observed *%SF_{fp}* with the estimated *%SF_{fp}* by Eq. 16, for all the Series of Overbank Flow

Series	Differential roughness, γ	Relative depth, β	Percentage of shear force carries by floodplains, %SF$_{fp}$	
			Observed	By Equation (16)
Smooth	1	0.279	81.23	85.39
	1	0.350	83.45	87.79
	1	0.365	83.88	88.22
	1	0.385	84.38	88.70
	1	0.412	84.99	89.32
Roughness I	1.12	0.279	80.95	85.39
	1.12	0.310	81.76	86.57
	1.12	0.328	82.19	87.14
	1.12	0.355	82.39	87.94
	1.12	0.385	82.91	88.70
	1.12	0.407	83.00	89.22
Roughness II	1.32	0.288	80.13	85.73
	1.32	0.317	80.88	86.79
	1.32	0.339	81.25	87.48
	1.32	0.364	81.48	88.19
	1.32	0.395	81.64	88.94
	1.32	0.410	81.64	89.27
Roughness III	1.47	0.275	79.18	85.21
	1.47	0.311	80.27	86.60
	1.47	0.339	80.79	87.48
	1.47	0.367	81.03	88.26
	1.47	0.388	81.15	88.78
	1.47	0.410	81.18	89.27

From the Table 12 it can be inferred that, due to the differential roughness effect, *%SF_{fp}* slightly decreases with the increase in differential roughness (γ). Therefore the difference factor of *%SF_{fp}* between the observed and the estimated value (by Eq. (16)), due to variation in differential roughness has been found out for all the series of experiment. The variation of difference factor with the parameter of relative depth (β) for different γ value is plotted in Fig. 5.5. To see the effect of γ on the *%SF_{fp}*, it was calculated from smooth curve equations (shown in Fig. 5.4), for a set of particular β value ($0.25 \leq \beta \leq 0.45$) for respective γ. The difference factor variation w.r.t. γ is plotted in Fig. 5.6. From the best fit functional relationship of the difference factor in Fig. 5.5 and 5.6, it

is clear that the difference factor is a logarithmic function of β and power function of γ which can be expressed as:

$$Difference\,factor = F_1(\gamma^{1.389}), F_2(\ln \beta) \tag{17}$$

where F_1 and F_2 are functional relationship. Eq. (17) indicates that $\%SF_{fp}$ is a logarithmic function of β and power function of γ in addition to the function of $\%A_{fp}$. Therefore, the Eq. (16) has been modified as:

$$\%SF_{fp} = 4.105\left[\frac{100\beta(\alpha-1)}{1+\beta(\alpha-1)}\right]^{0.6917} + 4.605\left[\frac{\gamma^{1.389}}{\ln \beta}\right] \tag{18}$$
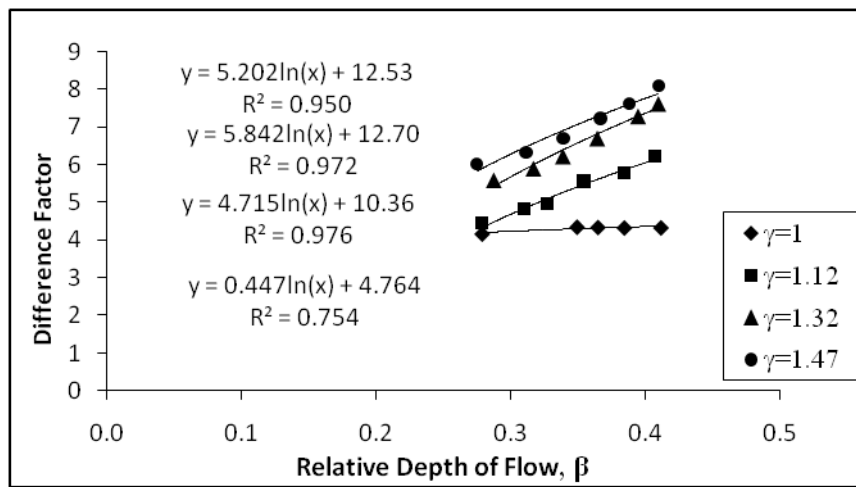

Fig. 5.5 Variation of difference factor of $\%SF_{fp}$ w.r.t. β for different γ values
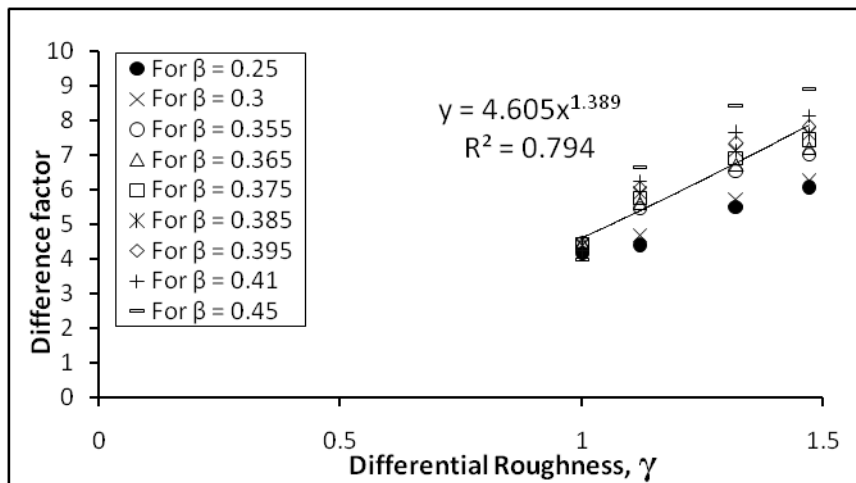

Fig. 5.6 Variation of difference factor of $\%SF_{fp}$ w.r.t. γ for different β values

The percentage error in estimating $\%SF_{fp}$ using Eq. (14), (15), (16) and (18) for recent data series are calculated by the following equation

60

$$\% \, Error = \frac{Estimated \, \% \, SF_{fp} - Actual \, \% \, SF_{fp}}{Actual \, \% \, SF_{fp}} \times 100 \tag{19}$$

The percentage error obtained for recent data series are shown in Fig. 5.7.1-5.7.4. The Eq. (18), as it is meant for homogeneous roughness, is compared only for smooth series (homogeneous roughness, $\gamma = 1$). From the graphs, it can be noted that the previous methods (Eq. (14) and (15)) of estimating $\%SF_{fp}$ in compound channels having non-homogeneous roughness, gives %error more than 20% , 30%, 35% and 40% for $\gamma = 1$, 1.12, 1.32 and 1.47 respectively with the present series of data, while the proposed method gives %error within ±1 for all.
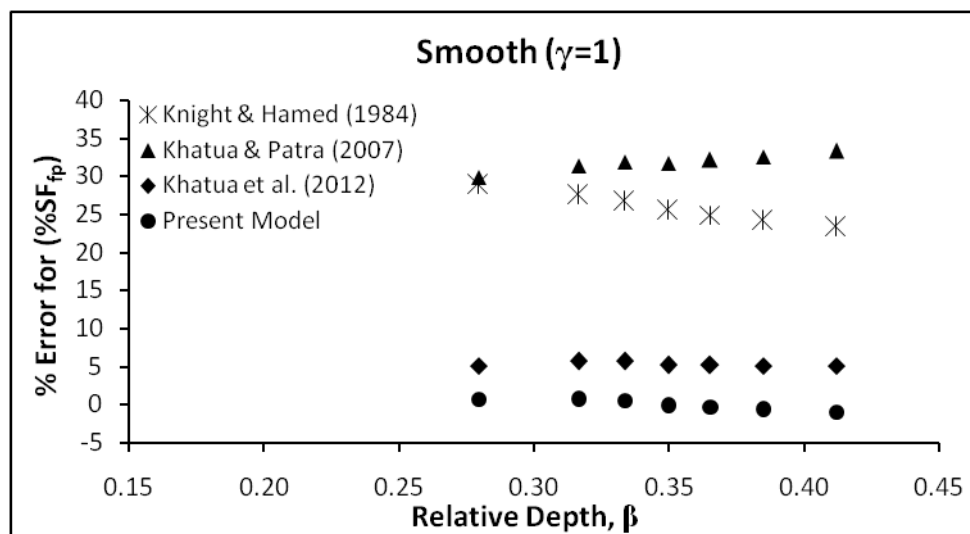

Fig. 5.7.1 %Error in Estimating *%SF_{fp}* for Smooth series
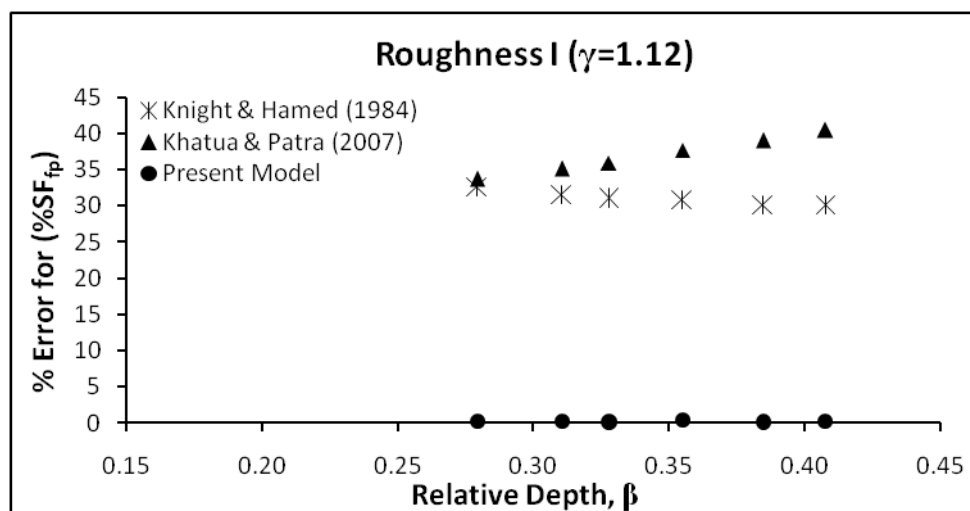

Fig. 5.7.2 %Error in Estimating *%SF_{fp}* for Roughness I series
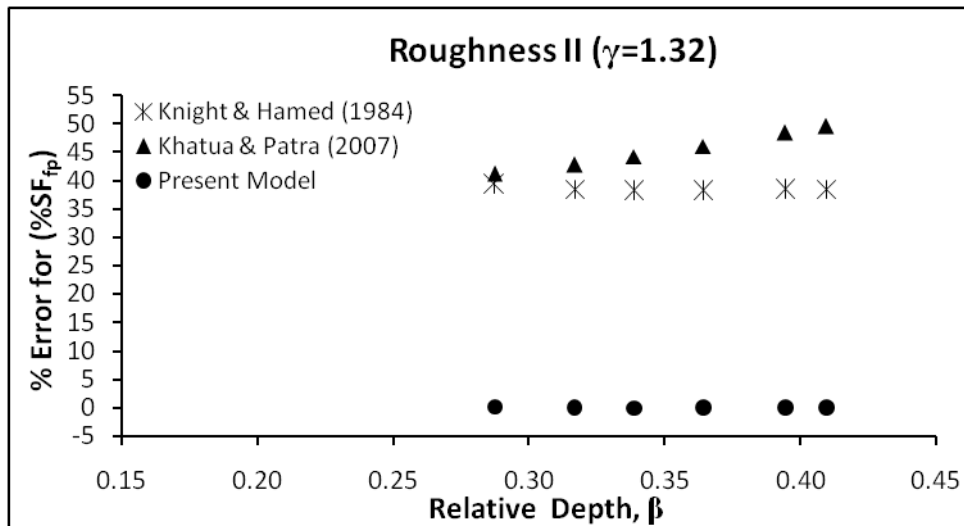
61

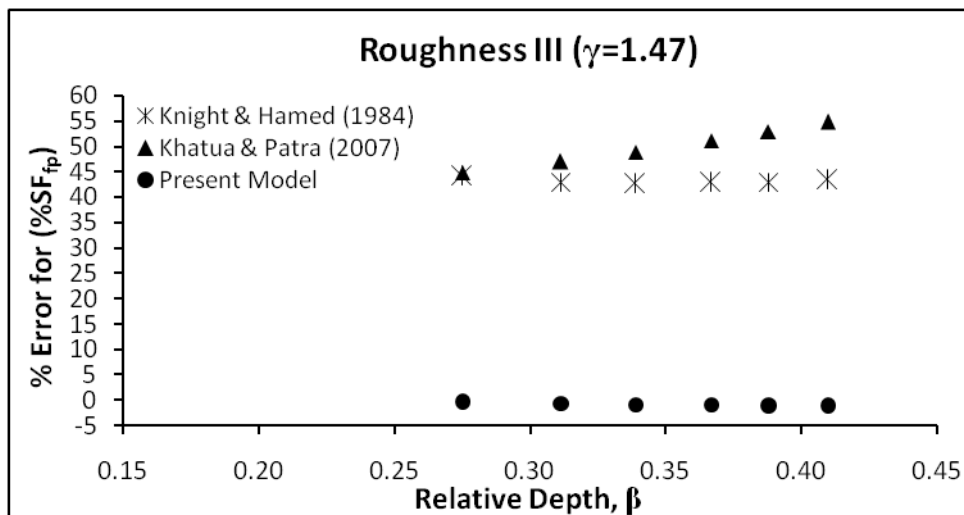**Fig. 5.7.3 %Error in Estimating *%SF$_{fp}$* for Roughness II series**

Fig. 5.7.4 %Error in Estimating *%SF$_{fp}$* for Roughness III series

Fig. 5.7 %Error in estimating *%SF$_{fp}$* by present and established methods for recent data series

For the validation test of Eq. (18), FCF data, Birmingham, UK, has been chosen as it is considered as the benchmark of laboratory experiment in hydraulics research and has been used by many investigators (Atabay and Knight (2002), Sellin et al. (2003), Abril, and Knight (2004), Yang et al. (2005), Yang et al. (2007), Moreta and Martin-Vide, (2010), Khatua et al. (2012)). FCF data, phase-A, series: 1,2,3,7,8 and 10 are choosen, as those were symmetric straight compound channels. In series 1,2,3,8 and 10, the surface of the compound cahnnel was smooth (i.e. homogeneously roughened, $\gamma = 1$); whereas in series 7, the suface was non homogeneously roughened and γ was 3.08 (Knight, 1990).

As the Khatua et al. (2012) method was developed for smooth compound channel (i.e. homogeneously roughened), it is not considered for comparision in series 7. The width ratio of all the compund channel in the series 1,2,3,8 and 10 were different; and that of series 7 was the same as in the series 10. For all these FCF series %error in estimating $\%SF_{fp}$ is calculated by using the present model (Eq. 18) for validation test. Then it is compared with the previous methods methods (Knight and Hamed, 1984; Khatua and Patra, 2007 and Khatua et al., 2012, i.e. Eq. (14), (15), (16) respectively). From the validation test the following observations are found.

- For smooth compound channel having low width ratio ($\alpha < 4$), the present model is found to give better results as compared to the other three previous methods (i.e. Knight and Hamed, 1984; Khatua and Patra, 2007 and Khatua et al., 2012) (Fig. 5.8.3).

- For $4 \leq \alpha \leq 4.4$, Knight and Hamed (1984) and Khatua and Patra (2007) methods are found to give poor result, whereas Khatua et al. (2012) and present model gives better results (Fig. 5.8.2, 5.8.5, 5.8.6).

- For $\alpha > 6$, Knight and Hamed (1984) method gives unrealistic result of shear force (i.e. %error around 100%) and Khatua and Patra (2007) method gives poor result; while Khatua et al. (2012) and present model gives good result (Fig. 5.8.1).

- But in case of non-homogeneously roughened compound channel (i.e. $\gamma = 3.08$), Knight and Hamed (1984) and Khatua and Patra (2007) failed (i.e. %error >100%); whereas the present model gives satisfactory result (Fig. 5.8.4).

This validation test of the present model (Eq. 18) with FCF data series is shown in the following Fig. 5.8 series.

Fig. 5.8.1 %Error in estimating *%SF*_{*fp*} by present and previous models for FCF series 1

Fig. 5.8.2 %Error in estimating *%SF*_{*fp*} by present and previous models for FCF series 2

Fig. 5.8.3 %Error in estimating *%SF*_{*fp*} by present and previous models for FCF series 3
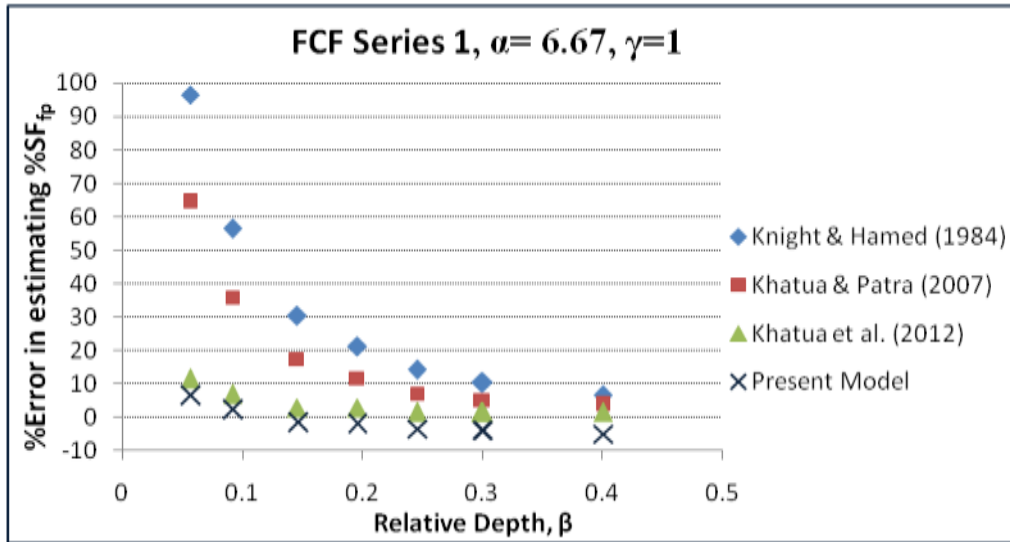
Fig. 5.8.4 %Error in estimating *%SF_{fp}* by present and previous models for FCF series 7
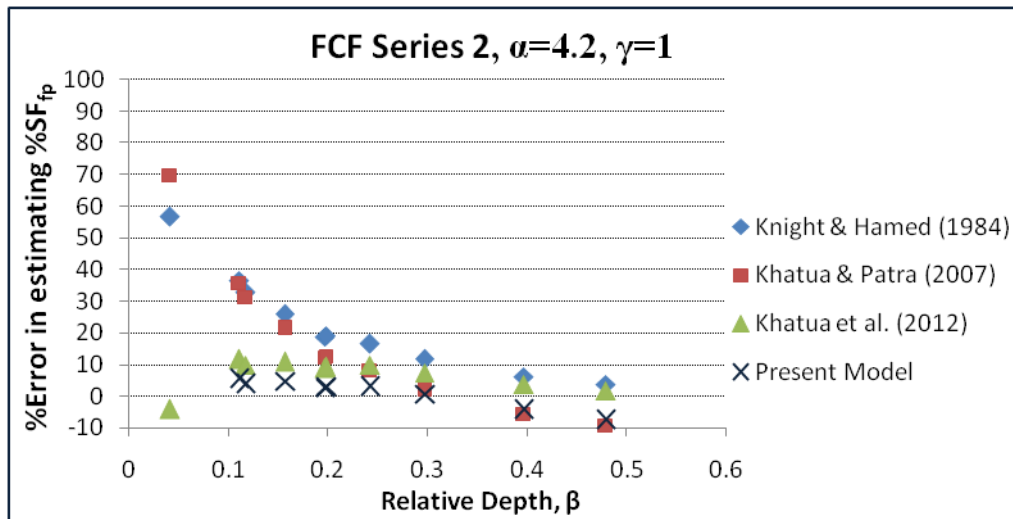

Fig. 5.8.5 %Error in estimating *%SF_{fp}* by present and previous models for FCF series 8
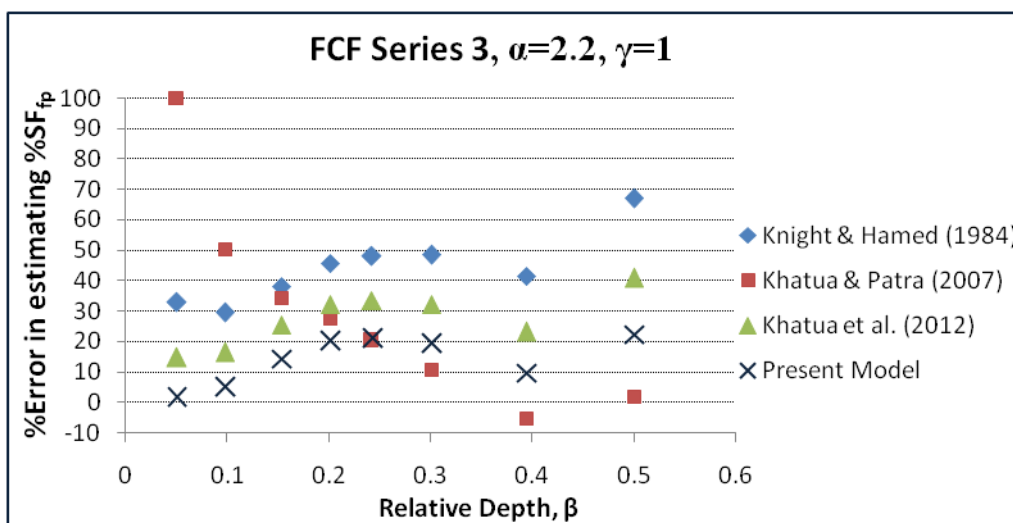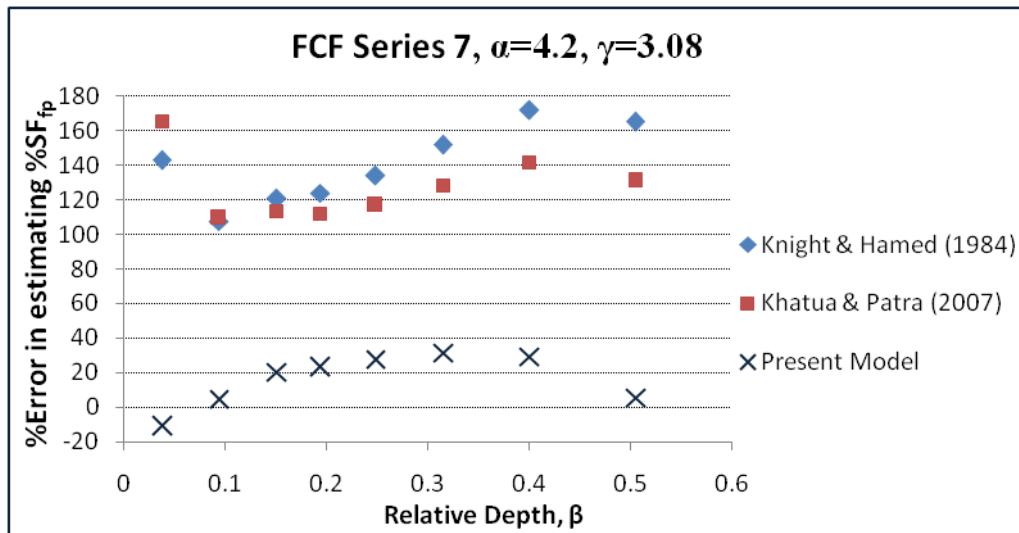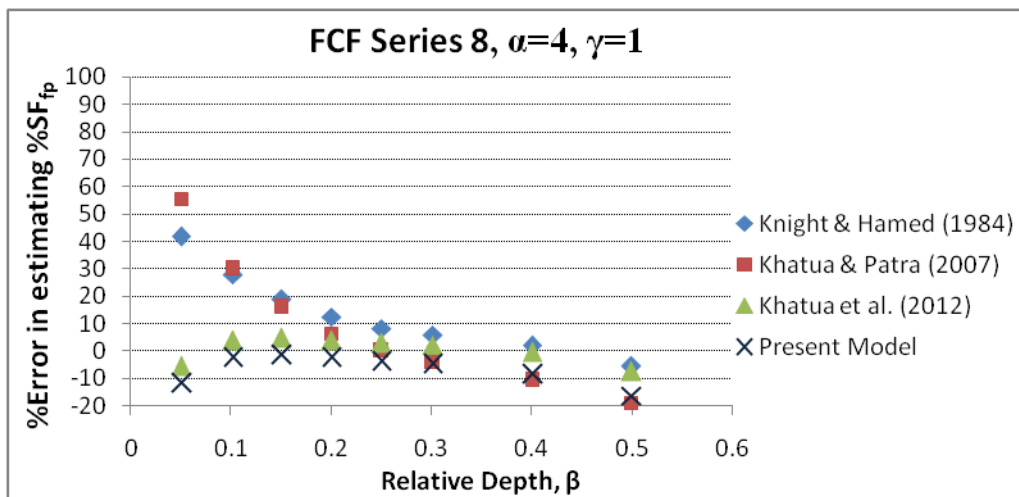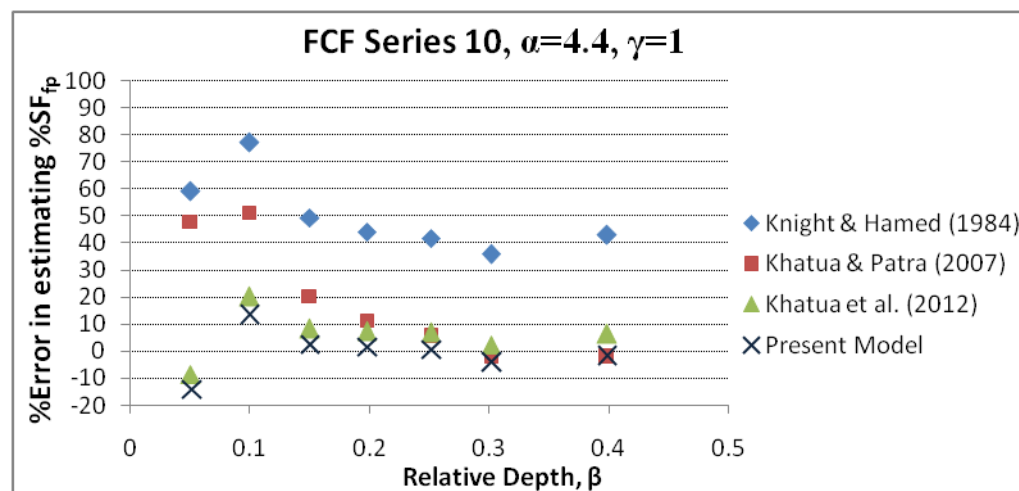

Fig. 5.8.6 %Error in estimating *%SF_{fp}* by present and previous models for FCF series 10

Fig. 5.8 Validation test of the proposed model with FCF data

Chapter 6

CONCLUSION

6   CONCLUSIONS

A series of laboratory experiments has been carried out to observe the effect of differential roughness on flow characteristics during overbank flow in a compound channel having high width ratio, from which the following conclusions can be drawn.

➢ From the results of stage-discharge relationship, it can be concluded that:

- The overall discharge found to increase with the increase in depth of flow and decrease with the increase in differential roughness, which may be attributed to the fact that at higher depth of flow, the effect of differential roughness as well as that of the momentum transfer between main channel and flood plain, decreases.

➢ From the observation of dimensionless stream-wise velocity isovels of contours, it can be concluded that:

- The concentration of maximum velocity contour is always found in main channel. The concentration found to decrease with the increase in depth of flow.

- The velocity variation on floodplain is found to be maximum for lowest depth of flow, then gradually stabilizing with the increase in depth of flow, whereas the variation is reverse in main channel.

- The overall range of variation in velocity is found to increase with the increase in differential roughness.

➢ From the observation of depth-averaged velocity, it can be noted that:

- Depth-averaged velocity in main channel region is found to increase with the increase in differential roughness and found to decrease in floodplain region with the increase in differential roughness.

- Depth-averaged velocity in main channel region found to decrease with the increase in relative depth of flow.

- The variation of depth-averaged velocity in main channel region and floodplain region found to increase with the increase in differential roughness.

➢ From the results of overall and zonal Manning's *n* distribution, it can be concluded that:

- The overall roughness coefficient, for overbank flow is found to increase with the increase in differential roughness value.

- The overall *n* suddenly decreases, when flow becomes inbank to overbank. Then again gradually increase with increase in depth of flow. The decrease of the overall *n* value in low depth overbank flow is mainly due to (i) sudden decrease in hydraulic radius and (ii) large amount of momentum transfer from main channel to floodplain. At higher overbank depths, the momentum transfer process is very less.

- The zonal roughness coefficient value of main channel is always found to be more than that of floodplain during the overbank flow.

- The zonal roughness coefficient of floodplain is found to increase with the increase in depth of flow.

➢ From the results of flow distribution, it can be concluded that:

- The percentage of flow in main channel is found to decrease with the increase in relative depth, as the effect of momentum transfer between floodplain and main channel decreases with the increase in depth of flow.

- The percentage of flow in main channel is found to increase with the increase in differential roughness, which may be attributed to that fact that the resistance to flow, offered by floodplain in comparison to main channel increases with the increase in differential roughness value (as main channel is smoother than floodplain).

➢ From the results of boundary shear distribution, it can be concluded that:

- The percentage of shear force carried by floodplains is found to increase with the increase in relative depth and decrease with the increase in differential roughness. This may be attributed to the possibility that the surface roughness, which reduces

the velocity of flow on floodplain resulting decrease in shear force (as shear force is dependent of velocity).

- A model has been derived using the present series of observed shear force data, for a straight and symmetrical compound channels having width ratio of 15.75; for differential roughness values of 1, 1.12, 1.32 and 1.47; and for relative depth range of 0.27 to 0.41.

- The proposed model is validated with the FCF data and compared with Knight and Hamed (1984), Khatua and Patra (2007) and Khatua et al. (2012) methods. From the test and comparison, it is found that the proposed model gives satisfactory result for homogeneously roughened as well as non-homogeneously roughened compound channel.

- The proposed model is quite appropriate for straight compound channel having $4 \leq$ width ratio ≤ 15.75, $0.1 \leq$ relative depth < 0.5 and $1 \leq$ differential roughness ≤ 15.67.

SCOPE FOR FUTURE STUDY

The present work leaves a wide scope for future investigators to explore many other aspects of differential roughness analysis.

- Flow characteristics like depth-averaged velocity, zonal n and overall n, flow distribution and boundary shear stress distribution have been performed for the low differential roughness value for a constant width ratio, which can be further analyzed for higher differential value.

- In the present study mesh and stone were used on the floodplain as roughening material which may be replaced by door mat, large stone size and the main channel can have either rigid or mobile bed.

- These flow characteristics can also be studied for different bed slopes and different width ratio.

- The equation developed for percentage shear force estimation, may be improved by incorporating more data of higher differential roughness. These data can be helpful for developing models by using theoretical as well as numerical approaches.

REFERENCES

REFERENCES

1. Abril, J.B. and Knight, D.W. (2004). "Stage-discharge prediction for rivers in flood applying a depth-averaged model". *J. Hydr. Res.*, *IAHR*, Vol. 42, No. 6, pp. 616-629.

2. Absi, R. (2011). "An ordinary differential equation for velocity distribution and dip-phenomenon in open channel flows". *J. Hydr. Res.*, *IAHR*, Vol. 49, No. 1, pp. 82-89.

3. Ackerman, J.D., Wong, L., Ethier, C.R., Allen, D.G. and Spelt, J.K. (1994). "Preston-static tubes for the measurement of wall shear stress". *J. Fluids Eng.,* Vol. 116, pp. 645–649.

4. Alhamid, A.I. (1991). "Boundary shear stress and velocity distribution in differentially roughened trapezoidal open channels". PhD thesis, The University of Birmingham, UK.

5. Al-Khatib, I.A., & Dmadi, N.M. (1999). "Boundary shear stress in rectangular compound channels". *Tr. J. Eng. and Environ. Sc.*, Vol. 23, pp. 9-18.

6. Abaza, K.A. and Al-Khatib, I.A. (2003). "Generalization of shear stress distribution in rectangular compound channels". *Tr. J. Eng. and Environ. Sc.*, Vol. 27, pp. 409-421.

7. Atabey, S. (2001). "Sediment transport in two stage channels". PhD Thesis, The University of Birmingham, U.K.

8. Atabay, S.A. and Knight, D.W. (2002). "The influence of floodplain width on the stage-discharge relationship for compound channels". *River Flow 2002*, Proc. Int. Conf. on Fluvial Hydraulics, Balkema, The Netherlands, Vol. 1, pp. 197-204.

9. Atabay, S. and Knight, D.W. (2006). "1-D modelling of conveyance, boundary shear and sediment transport in overbank flow". *J. Hyd. Res.* Vol. 44, No. 6, pp. 739–754.

10. Ayyoubzadeh, S.A. (1997). "Hydraulic aspects of straight compound channel flow and bedload sediment transport". PhD thesis, The University of Birmingham, England, U.K.

11. Babaeyan-Koopaei, K., Ervine, D. A., Carling, P. A. and Cao, Z. (2002). "Velocity and turbulence measurements for two overbank flow events in River Severn". *J. Hydr. Eng.*, *ASCE*, Vol. 128, No. 10, pp. 891–900.

12. Bhowmik, N. G., and Demissie, M. (1982). "Carrying capacity of floodplains". *J. Hydr. Div.*, *ASCE*, Vol. 108, No. 3, pp. 443-452.

13. Biron, P. M., Robson, C., Lapointe, M. F. and Guskin, S. J. (2004). "Comparing different methods of bed shear estimates in simple and complex flow fields". *Earth Surface Processes and Landforms*, 29, pp. 1403-1415.

14. Blanckaert, K., Duarte, A. and Schleiss A.J. (2010). "Influence of shallowness, bank inclination and bank roughness on the variability of flow patterns and boundary shear stress due to secondary currents in straight open-channels". *Advances in Water Resources*, Science Direct, Vol. 33, No. 9, pp. 1062-1074.

15. Chow, V.T. (1959). "Open-Channel Hydraulics". New York, McGraw- Hill Book Co.

16. Fernholz, H.H., Janke, G., Schober, M., Wagner P.M. and Warnack, D. (1996). "New developments and applications of skinfriction measuring techniques". *Meas. Sci. Technol.*, Vol. 7, pp. 1396–1409.

17. Ghosh, S., and Jena, S.B. (1971). "Boundary shear distribution in open channel compound". *Proceedings of the Institution of Civil Engineers, London, England*, Vol. 49, pp. 417-430.

18. Hin, L.S. and Bessaih, N. (2004). "Flow in compound channels". *1st International Confrence on Managing Rivers in the 21st Century*. Rivers 2004.

19. Hosseini, S.M. (2004). "Equations for discharge calculation in compound channels having homogeneous roughness". *Iranian Journal of Science & Technology*, *Transaction B*, Vol. 28, No. B5.

20. Joo, C.B.H. and Seng, D.M.Y. (2008). "Study of flow in a non-symmetrical compound channel with rough floodplain". *J. The Institution of Engineers*, *Malaysia*, Vol. 69, No.2, pp. 18-26.

21. Kean, J.W., Kuhnle, R. Smith, J.D., Alonso, C.V. and Langendoen, E.J. (2009). "Test of a method to calculate near-bank velocity and boundary shear stress". *J. Hydr. Eng.*, *ASCE*, Vol. 135, No. 7, pp. 588-601.

22. Khatua, K.K. & Patra, K.C. (2007). "Boundary shear stress distribution in compound open channel flow". *J. Hydr. Eng.*, *ISH*, Vol. 12, No.3, pp. 39-55.

23. Khatua, K.K. (2008). "Interaction of flow and estimation of discharge in two stage meandering compound channels". PhD Thesis, NIT, Rourkela, India.

24. Khatua, K.K., Patra, K.C. & Mohanty, P.K. (2012). "Stage-discharge prediction for straight and smooth compound channels with wide floodplains". *J. Hydr. Eng.*, *ASCE*, Vol. 138, No. 1, pp. 93-99.

25. Knight, D.W., and Demetriou, J.D. (1983). "Floodplain and main channel flow interaction". *J. Hydr. Eng., ASCE*, Vol.109, No.8, pp. 1073-1092.

26. Knight, D.W., and Hamed, M.E. (1984). ''Boundary shear in symmetrical compound channels.'' *J. Hydr. Eng.*, *ASCE*, Vol. 110, No. 10, pp. 1412-1430.

27. Knight, D.W. (1989). "Hydraulics of flood channels" in: *Floods: Hydrological, Sedimentological and Geomorphological Implications*. Beven, K. and Carling, P. (Eds.), John Wiley & Sons, Chichester, pp. 83 -105.

28. Knight, D.W. (1990). "Summary file and stage discharge results-Series 1–11 in SERC Flood Channel Facility Experimental Data-Phase A", Vol. 1. School of Civil Engineering, The University of Birmingham.

29. Knight, D.W. and Shino, K. (1996). "River channel and floodplain hydraulics." in *Floodplain Processes*. Anderson, M.G., Walling, D.E. and Bates, P.D. (Eds.), John Wiley & Sons, pp. Chichester, 139-181.

30. Knight, D.W., Tang, X., Sterling, M., Shiono, K. and McGahey, C. (2010). "Solving open channel flow problems with a simple lateral distribution model". *River Flow 2010*, Vol. 1, pp. 41-48.

31. Lambert, M.F. and Myers, W.R. (1998). "Estimating the discharge capacity in straight compound channels". *Proceedings of the Institution of Civil Engineers. Waters*, *Maritime and Energy*, Vol. 130, No. 2, pp. 84–94.

32. Maghrebi, M.F. and Rahimpour, M. (2006). "Streamwise velocity distribution in irregular shaped channels having composite bed roughness". *Flow Measurement and Instrumentation*, Science Direct, Vol. 17, No. 4, pp. 237–245.

33. Modi, P.N. and Seth, S.M. (1998). "Hydraulics and Fluid Mechanics". 12th Edition, Delhi, Standard Book House.

34. Moreta, P.J.M. and Martin-Vide, J.P. (2010). "Apparent friction coefficient in straight compound channels". *J. Hydr. Res.*, *IAHR*, Vol. 48, No. 2, pp. 169-177.

35. Myers, R. C., and Elsawy, E. M. (1975). "Boundary shear in channel with floodplain". *J. Hydr. Div., ASCE*, Vol. 101, No. 7, pp. 933–946.

36. Myers, W.R.C. (1987). "Velocity and discharge in compound channels". *J. Hydr. Eng.*, *ASCE*, Vol.113, No.6, pp. 753-766.

37. Myers, W.R.C. and Brennan, E.K. (1990). "Flow resistance in compound channels". *J. Hydr. Res.*, *IAHR*, Vol. 28, No. 2, pp. 141-155.

38. Myers, R.C. and Lyness, J.F. (1997). "Discharge ratio in smooth and rough compound channels". *J. Hydr. Eng.*, *ASCE*, Vol. 123, No. 3, pp. 182-187.

39. Myers, W.R.C., Lyness, J.F. and Cassells, J. (2001). "Influence of boundary roughness on velocity and discharge in compound river channels". *J. Hydr. Eng.*, *ASCE*, Vol. 39, No. 3, pp. 311-319.

40. Patel, V.C. (1965). "Calibration of the Preston tube and limitations on its use in pressure gradients". *J. Fluid Mech.*, Vol. 23, pp. 185-208.

41. Patel, P.L. and Ranga Raju, K.G. (1999). "Critical tractive stress of nonuniform sediments". *J. Hydr. Res.*, *IAHR*, Vol. 37, No. 1, pp. 39-58.

42. Preston, J.H. (1954) "The determination of turbulent skin friction by means of Pitot tubes". *J. Roy. Aeronaut. Soc.*, Vol. 58, pp. 109-121.

43. Rajaratnam, N. and Ahmadi, R.M. (1979). "Interaction between main channel and flood-plain flows." *J. Hydr. Div.*, *ASCE*, Vol. 105, No. 5, pp. 573-588.

44. Rantz, S. E. and others (1982). "Measurement and computation of streamflow: measurement of stage and discharge". *U.S. Geological Survey Water-Supply Paper 2175*, Vol. 1.

45. Rezaei, B. and Knight, D.W. (2011). "Overbank flow in compound channels with nonprismatic floodplains". *J. Hydr. Eng.*, *ASCE*, Vol. 137, No. 8, pp. 815-824.

46. Rice, C.E., Kadavy, K.C. and Robinson, K.M. (1998). "Roughness of loose rock riprap on steep slopes". *J. Hydr. Eng.*, *ASCE*, Vol. 124, No. 2, pp. 179-185.

47. Seckin, G. (2004). "A comparison of one-dimensional methods for estimating discharge capacity of straight compound channels". *Canad. J. Civil Eng.* Vol. 3, No. 4, pp. 619–631.

48. Sellin, R.H.J. (1964). "A laboratory investigation into the interaction between flow in the channel of a river and that of its flood plain". *La. Houilte Blanche*, No. 7, pp. 793-801.

49. Sellin, R.H.J., Bryant, T.B., Loveless, J.H. (2003) "An improved method for roughening floodplains on physical river models". *J. Hydr. Res.*, *IAHR*, Vol. 41, No. 1, pp. 3-14.

50. White, F.M. 1999. "Fluid Mechanics". 4th ed. WCB McGraw-Hill,Boston, Mass.

51. Wormleaton, P.R. and Hadjipanos, P. (1985). "Flow distribution in compound channels". *J. Hydr. Eng.*, *ASCE*, Vol. 111, No. 2, pp. 357-361.

52. Yang, S.Q. and Lim, S.Y. (1998). "Boundary shear stress distributions in smooth rectangular open channel flows". *Proceedings of the Institution of Civil Engineers. Waters*, *Maritime and Energy*, Vol. 130, No. 3, pp. 163–173.

53. Yang, S.Q., Tan, S.K., Lim, S.Y. (2004). "Velocity distribution and dip-phenomenon in smooth uniform open channel flows". *J. Hydr. Eng.*, *ASCE*, Vol. 130, No. 12, pp. 1179-1186.

54. Yang, K., Cao, S. and Liu, X. (2005). "Study on resistance coefficient in compound channels". *Acta Mech Sin*, Springer-Verlag, Vol. 21, pp. 353-361.

55. Yang, K., Cao, S. and Liu, X. (2007). "Flow resistance and its prediction methods in compound channels". *Acta Mech Sin*, Springer-Verlag, Vol. 23, pp. 23-31.

56. Zheleznyakov, G.V. (1971). "Interaction of Channel and Floodplain Streams". *Proc. 14th Congress of IAHR,* Vol. 5, Paris, France, pp. 144-148.

[i]. http://www.flowdata.bham.ac.uk/atabay/index.shtml.

[ii]. http://www.flowdata.bham.ac.uk/tang/data.shtml

[iii]. http://www.trekearth.com/gallery/Asia/India/South/Andhra_Pradesh/Rajamundy/photo546682.htm

[iv]. http://www.unp.me/f143/indus-river-images-detail-pakistan-china-india-161408/

[v]. *Indian Standard,* Methods of Test for Aggregates for Concrete, Part I, Particle Size and Shape, IS: 2386 (Part I) – 1963 (Reaffirmed 2007).

[vi]. *Indian Standard,* Methods of Test for Aggregates for Concrete, Part III, Specific Gravity, Density, Voids, Absorption and Bulking, IS: 2386 (Part III) – 1963 (Reaffirmed 2002).

[vii]. *Indian Standard,* Methods for Test Sieving, IS: 1607 – 1977 (Reaffirmed 2001).

Publications

From this work

1. "Distribution of Boundary Shear in Compound Channel with Rough Floodplains" This paper is accepted for ninth International Conference in Advances in Fluid Mechanics, June 2012, AFM-2012, Split, Croatia.

2. "Effect of Differential Roughness on Boundary Shear Distribution in Compound Open Channel Flow" This paper is communicated in Journal of Flow Measurements and Instrumentation, Science Direct, Elsevier.

From other related work

3. "Evaluation of Boundary Shear in Meandering Channels" This paper is published in the proceedings of ninth International Conference on Hydro-Science and Engineering by IAHR and IIT Madras, (ICHE 2010), 2 - 5 August 2010.

4. "Stage-Discharge Prediction for Meandering Channels" This paper will be published in the International Journal of Computational Methods and Experimental Measurements, Wit press journal, Southampton, UK, in September 2012.

Brief Bio-data of the Author

NAME : NIRJHARINI SAHOO

FATHER'S NAME : Dr. PURNA CHANDRA SAHU

MOTHER'S NAME : Mrs. SAUDAMINI SAHOO

HUSBAND NAME : Mr. TUSAR RANJAN SAHOO

DATE OF BIRTH : 21-05-1982

NATIONALITY : INDIAN

PRESENT ADDRESS : M.TECH (RESEARCH),
DEPT. OF CIVIL ENGINEERING,
NATIONAL INSTITUTE OF
TECHNOLOGY, ROURKELA -
769008

PERMANENT ADDRESS C/o Dr. RAMESH CHANDRA SAHOO
At: DHARITRI NAGAR,
SAMARAYPUR
P.O: GELPUR
Via: MADHAB NAGAR
Dist: BHADRAK
PIN: 768100

EDUCATIONAL QUALIFICATIONS :B.TECH, CIVIL ENGINEERING,2004

+2 SCIENCE, 1999

H. S. C., 1997